Quantum Chemistry and Molecular Engineering of Oligomeric and Polymeric Materials for Optoelectronics

JEAN-MARIE ANDRÉ* and JOSEPH DELHALLE

Laboratoire de Chimie Théorique Appliquée, Facultés Universitaires Notre-Dame de la Paix, Rue de Bruxelles, 61 B-5000 Namur, Belgium

Received January 2, 1991 (Revised Manuscript Received May 6, 1991)

Contents

I. Introduction

Materials which exhibit high linear and nonlinear responses are currently the subject of intense and worldwide research activities. Both linear and nonlinear responses find important scientific and technological applications, but nowadays the nonlinear electric responses receive much of the interest owing to their promises in telecommunications. Optical communication characterized by high data-transmission rates free from electrical interference, dynamic image processing (night vision, phase conjugation, pattern recognition, etc.), and optical computing are three examples where optical technologies are expected to gradually take over electronic techniques. For these applications, devices with a nonlinear optical medium are needed to control light electrically and optically.

At least, three types (multilayered semiconductor structures, inorganic, and organic compounds) of materials can be chosen for integration in optoelectronic devices; they all have advantages and shortcomings.[1] The growing interest in organics stems from many facts.[2] First of all, they are comparatively cheap and easy-to-process materials. Furthermore, due to the specific role played by the carbon atom in chemistry, it is relatively simple to optimize the materials by modifying known molecular structures and/or creating new ones. Finally and most important, some organic compounds have shown enhanced electric responses over a wide frequency range, ultrafast response times, and high laser-damage thresholds.

High electric susceptibilities very much depend on the nature of the delocalized structure and it is the purpose of a molecular design in optoelectronics to find molecular systems that yield the largest possible responses because, among other conditions and advantages, the larger these linear and nonlinear responses and the smaller the electric field required to achieve the desired electrooptic effect. As already pointed out, the molecular structure of organic materials can easily be modified in order to maximize the electric responses, but this versatility also raises problems because, due to cost and time, it is practically impossible to prepare and test all interesting compounds. Quantum chemistry can help in this type of endeavour not only by rationalizing experimental results but also by ranking existing molecular structures according to their polarizability and hyperpolarizabilities prior to experiment and propose the preparation of new promising compounds to the chemists.

In this contribution, we want to describe some of our efforts in using quantum chemistry methods to search for promising monomeric structures that could be incorporated in active main-chain polymers. The paper is organized as follows: in section II, we briefly introduce a minimal number of concepts about optical linearities and nonlinearities; in section III, a short account on the most important forms of electroactive organic materials is given with special emphasis on the active main-chain polymers. Section IV describes the method of calculation used in our illustrations (section V) of quantum chemistry applied to the optoelectronics field. As explained in section V, reliable calculations of second hyperpolarizability coefficients are essentially restricted to very small systems. Since this is where the interest for active main-chain resides, we rely in this work on linear response calculations as indicative of trends for nonlinear responses. Section VI serves as an introduction to problems raised by the quantum chemistry treatment of infinite polymers. Concluding remarks, especially on the presently weak points of the theory, are made in section VII.

II. Optical Linearities and Nonlinearities

When an electromagnetic wave propagates through a medium, it induces a polarization **P** and a magnetization **M** as a result of the motion of the electrons and nuclei in response to the applied fields. We are inter-

0009-2665/91/0791-0843$09.50/0

A native of Belgium, Jean-Marie André received B.Sc. (1965) and Ph.D. (1968) degrees from the Catholic University of Louvain (UCL). After successively being research assistant and senior research associate of the Belgian National Fund for Scientific Research (FNRS), he became Associate Professor of Chemistry at the "Facultés Universitaires Notre-Dame de la Paix" in Namur, where he established the theoretical chemistry laboratory with a primary interest in the field of the electronic properties of polymers. André has been the director of this laboratory since 1974 and was promoted to full professor the same year. He served as chairman of the chemistry department from 1980 to 1983. André has written about 190 scientific papers and five books. An original monography on the quantum theory of polymers has been recently completed with J. Delhalle and J. L. Brédas and published by World Scientific Publishing Co. Among his awards can be mentioned the Empain prize of the Belgian University Foundation (1970), the Agathon de Potter award of the Royal Academy of Belgium (1979), the triennal award of the Belgian Chemical Society (1983), the annual medal of the International Academy of Molecular Quantum Science (1984), a distinction granted for his innovative contribution to the development of the quantum chemistry of polymers, and the Francqui prize (1991), the highest Belgian scientific distinction.

Born in Belgium, Joseph Delhalle received his B.Sc. (1969) and Ph.D. (1972) degrees from the Catholic University of Louvain (UCL). He has successively been research assistant and senior research associate of the Belgian National Fund for Scientific Research (FNRS). In 1972 he joined Prof. Jean-Marie André's laboratory at the "Facultés Universitaires Notre-Dame de la Paix" in Namur. In 1978 he became Associate Professor of Chemistry and Professor in 1986. He is present the Chairman of the Chemistry Department. Delhalle has written about 150 scientific papers; he is the coeditor of three books and coauthor of a recent monograph on the quantum theory of polymers. He has been appointed Visiting Professor of Chemistry at the University of Utah (1982) and at the Ecole Normale Supérieure (Paris) in 1984 and 1985.

ested only in the induced polarization and it is only for the purpose of keeping the general equations in their familiar form that in the sequel, we will occasionally refer to the magnetization. The induced polarization oscillates at frequencies determined by a combination of the properties of the material and the frequencies contained in the incident light waves. The optical properties of the medium and the characteristics of the radiation that is transmitted through the medium result from interactions between the fields radiated by the induced polarizations and the incident fields.

At low field intensities, the induced polarization is proportional to the applied electric field intensity, and the response of the medium is linear. Various linear optical interactions can occur, depending on the specific properties of the induced polarizations. Examples of linear processes are Rayleigh, Raman, and Brillouin scatterings. When the intensity of the incident radiation is high enough, the nature of the response of the medium changes, leading to the nonlinear optical effects. Some nonlinear optical interactions arise from the more extended motion of the electrons and ions in response to the stronger optical fields. Examples of this type nonlinear optical processes are harmonic generation and parametric frequency mixing. A second type of nonlinear response results from a change in the property of the medium caused by the incident wave, which in turn affects the propagation of the wave. An example of such a response is a change in the refractive index of a medium induced by the optical wave.

The propagation of an optical wave in a medium is described by the Maxwell equation for the electric field, the effects of the induced polarizations and magnetizations being included, together with relations defining the dependence of the induced polarizations and magnetizations with the optical field. The Maxwell equation for the electric field of an optical wave in a medium is[3]

$$\nabla^2\mathbf{E}(\mathbf{r},t) - (\epsilon_0\mu_0)\frac{\partial^2\mathbf{E}(\mathbf{r},t)}{\partial t^2} = \mu_0\frac{\partial^2\mathbf{P}(\mathbf{r},t)}{\partial t^2} + \frac{\partial[\nabla \times \mathbf{M}(\mathbf{r},t)]}{\partial t} \quad (1)$$

$\mathbf{E}(\mathbf{r},t)$ is the macroscopic electric field; it is the total electric field in the medium, arising both from the optical wave and from the induced polarization, averaged over domains that are large compared with molecular dimensions.[3d] $\mathbf{P}(\mathbf{r},t)$ and $\mathbf{M}(\mathbf{r},t)$, respectively, are the induced polarizations and magnetizations describing the effect of a medium present in the propagation path.

The problem of propagation in a medium is completely specified when the relations (constitutive relations) between the polarization and magnetization and the optical field are given. In the area of optoelectronics, assumptions can be made[3b] that lead to an expansion of the induced polarization in a power series in the electric field of the light wave of the form

$$P_i(\mathbf{r},t) = \epsilon_0\{\sum_j \chi_{ij}^{(1)}E_j(\mathbf{r},t) + \sum_{jk}\chi_{ijk}^{(2)}E_j(\mathbf{r},t)E_k(\mathbf{r},t) + \sum_{jkl}\chi_{ijkl}^{(3)}E_j(\mathbf{r},t)E_k(\mathbf{r},t)E_l(\mathbf{r},t) + ...\} \quad (2)$$

where the indices i, j, k, and l label the x, y, and z components of the vector and tensor quantities occurring in eq 2. The coefficients $\chi_{ij...}^{(n)}$ are the nth-order electric susceptibilities; the first-order susceptibilities describe the linear optical effects, while the remaining terms describe the nth-order nonlinear optical effects. As suggested by their index notation, the susceptibilities are tensors; they relate components of the nonlinear polarization vector to the various components of the optical field vectors.

Expression 2 is valid when the optical fields are weak compared to the electric field responsible for the binding of the electrons in the material. Also, the wavelength of the radiation must be long compared to the dimension of the atoms and molecules of the nonlinear medium, so that a multipole expansion can be used. For most nonlinear optical interactions, the electric dipole susceptibilities are the dominant terms because the wavelength of the radiation is usually much longer than the scattering centers. In line with Neumann's principle, which states that the physical properties of a system are invariant to its symmetry operations, the susceptibility tensors $\chi_{ij...}^{(n)}$ have the symmetry properties of the medium and thus can restrict the combinations of vectors components of the various optical fields that could practically be used. For instance, the odd susceptibility terms are always nonzero, while the even terms can be vanishing due to centrosymmetry. Thus to have effects driven by second-order nonlinear susceptibility terms it is important to have a noncentrosymmetric medium.

In order to make quantum chemistry useful in optoelectronics problems one needs to bring, and to some extent reduce, the problem down to the microscopic level. The molecular response relates the change in the molecular dipole moment, **p**, upon interaction with a field, **F**, as[3d]

$$p_i(t) = \sum_j \alpha_{ij} F_j(\mathbf{r},t) + \sum_{jk} \beta_{ijk} F_j(\mathbf{r},t) F_k(\mathbf{r},t) + \sum_{jkl} \gamma_{ijkl} F_j(\mathbf{r},t) F_k(\mathbf{r},t) F_l(\mathbf{r},t) + \ldots \quad (3)$$

where the indices i, j, k, and l label the x, y, and z components with respect to the reference frame in which the molecular system is described. Here $p_i(t)$ is the time-dependent ith component of the induced dipole moment vector $\mathbf{p}(t)$; α_{ij}, β_{ijk}, and γ_{ijkl} are the components of the molecular linear polarizability, first hyperpolarizability, and second hyperpolarizability tensors, respectively. For molecules in the bulk, e.g. in a crystal environment, the use of eq 3 is not trivial because the polarizing field **F** differs from the applied optical field and the molecular response is not that of the isolated compound. In spite of these problems and because large intrinsic values of the coefficients α_{ij}, β_{ijk}, and γ_{ijkl} are necessary conditions for high macroscopic electric responses to exist, it is quite useful to study isolated systems and compare their calculated response. In the case of organics, for example, high electric responses have invariably been noted in systems containing delocalized π electrons. Out of possible conjugated structures, many can readily be discarded on the basis of simple considerations (number of π electrons, chain length, etc.), but more quantitative assessments require direct quantum mechanical calculations of the coefficients α_{ij}, β_{ijk}, and γ_{ijkl}. Factors such as structure, primary and secondary, and the resulting electron-density distribution turn out to have a great influence on these properties and are hardly predictable from rules of thumb.

For an isolated compound in an applied electric field, the polarizability and hyperpolarizabilities are the free-compound properties which can be calculated by quantum chemistry methods. In this contribution only the time-independent (static or frequency-independent) molecular responses will be considered. They can be calculated by taking the derivatives of the induced dipole moment, **p**, of the system:

$$\alpha_{ij} = \left[\frac{\partial p_i}{\partial F_j}\right]_{F=0} \quad (3a)$$

$$\beta_{ijk} = \tfrac{1}{2}\left[\frac{\partial^2 p_i}{\partial F_j \partial F_k}\right]_{F=0} \quad (3b)$$

$$\gamma_{ijkl} = \tfrac{1}{6}\left[\frac{\partial^3 p_i}{\partial F_j \partial F_k \partial F_l}\right]_{F=0} \quad (3c)$$

Section IV is devoted to a brief description of the calculation methods applied to the systems considered in this work. However, before addressing this question, it is appropriate to briefly describe the class of compounds that will be considered in this review and indicate why quantum chemistry calculations can be valuable in the area of active main-chain polymers.

III. Active Main-Chain Polymers

To be useful for integration in linear and nonlinear optical devices, materials must combine, in addition to high molecular electric susceptibilities, many other properties such as a suitable organization at the molecular level with possible restrictions on symmetry, chemical stability, appropriate transparency regions, etc. Like in drug design, the conception of new compounds for optoelectronics is a complex task where these many constraints on the prospective system must be met simultaneously before a good material can be claimed. Moreover, since the classes of compounds used to form materials often depend on the particular application, it is expected that there will be a continuous need for designing new compounds for optoelectronics. Owing to the current attraction for nonlinear optical materials, we briefly indicate the most important forms in which they occur. However, it should be kept in mind that materials based on linear responses retain their full interest and the results reported in this contribution are also valuable for that class of materials.

The most important forms of organic nonlinear materials so far produced are single crystals, Langmuir–Blodgett films, active side-chain polymers where the active molecules are *grafted* to the polymer backbone, and active main-chain polymers in which the active groups are *incorporated into* the polymer backbone. Impressive optical-quality single crystals of several materials[4] are now available and can be used in harmonic generators, parametric amplifiers, etc. However crystal growth and material engineering (cutting and optical polishing) are still challenging problems to solve toward technological applications. Langmuir–Blodgett film deposition[5] is a very attractive technique to organize layers of active molecules and impose symmetry constraints dictated by $\chi^{(2)}$ effects. However, producing Langmuir–Blodgett films of good optical quality with sufficient stability remains a major target. This is why a large body of the efforts in the nonlinear optics area have been devoted to polymers.

Active side-chain polymers[6] are presently very attractive organic materials for $\chi^{(2)}$ effects because they offer the best compromise between nonlinear optical

properties and processing characteristics. In particular, they are quite amenable to electric field poling to remove centrosymmetry by aligning the permanent dipoles of the side chains with an externally applied electric field. As a result, active side-chain polymers have developed rapidly and simple integrated electrooptical devices with commercially interesting specifications are being proposed. Optimization of these materials is still needed; the major efforts being to increase the density and orientation of optically active species as well as to improve the time and temperature stability of the nonlinear optical effects imparted to the films by the poling process.

Active main-chain polymers[1,2f,7] offer the possibility of larger concentrations of active groups, chemically linked together into the polymer backbone and possibly conjugated over large distances. Even though attempts have been made to remove centrosymmetry in such polymers by poling techniques, they are more naturally interesting for $\chi^{(3)}$ effects where noncentrosymmetry is not required. Scaling rules predict that the linear molecular polarizability should scale with the conjugation length l_π to the third power, l_π^3, whereas the molecular second hyperpolarizability should increase with the fifth power of that quantity, l_π^5. On the basis of these guidelines, early efforts have been directed toward structures exhibiting increased delocalization length of π-electron networks to enhance the molecular second hyperpolarizability. Various conjugated polymers have been proposed and tested, so far with limited success because gap lowering and increased coloration have always been the consequences of an enhanced delocalization. Such consequences are strongly conflicting with transparency requirements and with other needed properties such as chemical stability, light scattering, etc., and it looks as if long conjugation sequences are not really appropriate to meet requirements for devices. This is why, for instance, copolymerization of conjugated oligomeric active segments with saturated spacer units has recently been investigated.[8] This combination of active and nonactive moieties has various advantages: control of the conjugation length and optical characteristics of the optically nonlinear active repeat units as well as increased processability and film-forming capability by controlling the length and chemical composition of the saturated spacer(s). If high electric responses in conjugated organic systems depend directly on the chemical nature of the delocalized networks, they also depend on their configurational and conformational structure in the bulk. Controlling the molecular architecture and increasing the density of active species appears thus as an important part of the molecular design of new materials for third-order nonlinearities. In view of the abovementioned requirements, it comes as no surprise if crystalline polydiacetylene derivatives are still among the best polymeric systems known to date.

This very brief introductory account on the active main polymers for nonlinear optics illustrates that it is a truly challenging area, and chemical ingenuity will probably be the key to success. Quantum chemistry can be valuable to this endeavor. Not only can it provide calculated molecular polarizability and hyperpolarizabilities of new interesting compounds (monomers, oligomers, and polymers) but alo use the full register of its predictive potentialities to address many of the chemical questions arising in this context (prediction of equilibrium geometry, most stable conformations, and configuations; analysis of the chemical bonding and rationalizing the changes in (hyper)polarizabilities; calculation of the extent of bond length alternations due to chemical substitution or charge transfer complexation; comparison of the stability of molecular complexes or isomeric structures; etc.). A short and therefore nonexhaustive account of a selection of our early and present quantum chemistry contributions in this domain is presented in section V.

Before proceeding with illustrations based on our own results, it is in order to provide a brief and necessarily incomplete account of the theoretical efforts made in the area of electric response in direct or distant connection with optoelectronics. Prior to the increasing number of calculations for optoelectronids, Hameka was the first to get trends of electric responses in a series of related conjugated molecules.[9] Flytzanis and coworkers[10] have contributed much to clarify the problem relating to infinite systems and contributed to help identify the dependence of electric responses on the dimensionality of the systems (scaling laws). Other important contributions made at the π-electron level are due to Ratner,[11] Beratan,[12] Wagnière,[13] and their respective co-workers.

Many semiempirical calculations have also been published. Zyss and collaborators[14] were the first to rely in a systematic way on quantum chemistry methods to assess the relative merits of specific molecular structures and the influence of substituents on the electric responses. They were able to predict the optical nonlinearities of a large variety of molecules and relate these values to other properties such as the transparency region and the degree of polarity of the excited charge transfer states. Other groups were also actively using semiempirical methods with the goal of identifying and designing materials with high electric responses: Garito,[15] Morley,[16] Waite,[17] Pierce,[18] Svendsen,[19] Zerner,[20] Williams,[21] and their co-workers.

The works made at the ab initio level can be divided in two classes: the highly accurate calculations mostly carried out on atomic and diatomic systems and those performed on relatively complex molecules. In the first group are, among others, Bishop,[22] Shelton,[23] Thakkar,[24] Oddershede,[25] Jørgensen,[26] and their co-workers. In the other group are the works on more complex systems which therefore can only rely on less sophisticated methods and thus aim at qualitatively reliable numbers. Beside our own contributions which will be illustrated in section V, one can mention the works by Kirtman,[27] Dupuis,[28] and their co-workers.

These works have been the primary source of inspiration for our own contribution; other important contributions have surely been omitted and we must apologize for this.

IV. Methods of Calculation

Reported calculations are at the Hartree–Fock level. The finite field–self-consistent field (SCF–FF) method we use in the oligomeric calculations described in this paper was originally proposed by Cohen and Roothaan[29] and is equivalent to an analytic coupled Hartree–Fock scheme, standing out for its simplicity.

In the SCF technique, one assumes an independent particle model in the form of an approximate many-electron wave function and utilizes the variation theorem. The simplest independent particle wave function for an n-electron system is a simple product of n orbitals. However, such a form does not include the spin properties and does not satisfy the Pauli exclusion principle. Thus, in order to take into account these requirements, an antisymmetrized product of n spin orbitals, called a Slater determinant, is used. A four-variable spin orbital $\Phi_i(\mathbf{r},\omega)$ is the product of a spatial orbital $\phi_i(\mathbf{r})$ and of a spin function $\sigma(\omega)$, which can be either $\alpha(\omega)$ or $\beta(\omega)$. The HF equation is the one-electron equation which allows us to obtain the best orbitals, i.e., those spin orbitals that, introduced in an antisymmetrized product of spin orbitals, give the best total energy of the system (the lowest and the closest to the experimental value in agreement with the variation principle) which can be obtained from such a wave function. These equations were suggested independently by the Englishman Hartree,[30] the Russian Fock,[31] and the American Slater.[32] Different versions of the Hartree–Fock theory have been proposed to deal more conveniently with the specific nature of the systems considered (closed shell, open shell). The closed-shell approximation forces the electrons to be paired in common spatial orbitals. The oligomers and polymers we consider in this paper are most often in such situation and therefore we consider only the closed-shell approximation.

The one-electron Hartree–Fock operator has the form

$$h_0(\mathbf{r}) = -\tfrac{1}{2}\nabla^2 - \sum_A \frac{Z_A}{|\mathbf{r} - \mathbf{R}_A|} + \sum_j^{\text{occ}}\{2J_i(\mathbf{r}) - K_j(\mathbf{r})\} \quad (4)$$

where the Coulomb repulsion and exchange interaction operators are defined by the equations

$$J_j(\mathbf{r})\ \phi_i(\mathbf{r}) = \left\{\int d\mathbf{r}'\phi_j(\mathbf{r}')\phi_j(\mathbf{r}')|\mathbf{r} - \mathbf{r}'|^{-1}\right\}\phi_i(\mathbf{r}) \quad (5a)$$

$$K_j(\mathbf{r})\ \phi_i(\mathbf{r}) = \left\{\int d\mathbf{r}'\phi_j(\mathbf{r}')\phi_i(\mathbf{r}')|\mathbf{r} - \mathbf{r}'|^{-1}\right\}\phi_j(\mathbf{r}) \quad (5b)$$

We note the underlying physical meaning of the HF field: one determines the motion of a single electron characterized by the kinetic operator $-\tfrac{1}{2}\nabla^2$ in the electrostatic field of fixed nuclei $\{-\sum_A Z_A|\mathbf{r} - \mathbf{R}_A|^{-1}\}$. The electron also moves in the interaction field due to its repulsion Coulomb operator $\{\sum_j^{\text{occ}} 2J_j(\mathbf{r})\}$ with the average electron density $\{\sum_j \phi_j(\mathbf{r}')\phi_j(\mathbf{r}')\}$ and the exchange interaction $\{\sum_j^{\text{occ}} K_j(\mathbf{r})\}$. In the linear combination of atomic orbitals (LCAO) scheme, the molecular orbitals are expanded in terms of atomic functions

$$\phi_j(\mathbf{r}) = \sum_p c_{jp}\chi_p(\mathbf{r}) \quad (6)$$

The numerical evaluation of the matrix elements of $h_0(\mathbf{r})$ requests the calculation of one-electron overlap (S_{pq}), kinetic (T_{pq}), and nuclear attraction ($V_{pq|A}$) integrals

$$S_{pq} = \int \chi_p(\mathbf{r})\chi_q(\mathbf{r})d\mathbf{r} \quad (7a)$$

$$T_{pq} = \int \chi_p(\mathbf{r})\{-\tfrac{1}{2}\nabla^2\}\chi_q(\mathbf{r})d\mathbf{r} \quad (7b)$$

$$V_{pq|A} = \int \chi_p(\mathbf{r})\frac{1}{|\mathbf{r} - \mathbf{R}_A|}\chi_q(\mathbf{r})d\mathbf{r} \quad (7c)$$

two-electron integrals

$$(pq|rs) = \int\int \chi_p(\mathbf{r})\chi_q(\mathbf{r})\frac{1}{|\mathbf{r} - \mathbf{r}'|}\chi_r(\mathbf{r})\chi_s(\mathbf{r})d\mathbf{r}d\mathbf{r}' \quad (8)$$

and varying iteratively combinations of LCAO coefficients (density matrix elements D_{pq}):

$$D_{rs} = \sum_j^{\text{occ}} c_{jr}c_{js} \quad (9)$$

In the finite field–self-consistent field (SCF–FF) technique, a term, $e\mathbf{r}\cdot\mathbf{F} = -\mathbf{r}\cdot\mathbf{F}$ in au, describing the interaction between the external field, $\mathbf{F}$, and the elementary charges (electrons and nuclei constituting the molecule) is added to the molecular Hamiltonian; at this level, the orbitals are self-consistent eigenfunctions of the one-electron field-dependent Fock operator, $h(\mathbf{r})$:

$$H^{\text{FF-SCF}}(\mathbf{r}) = -\tfrac{1}{2}\nabla^2 - \sum_A Z_A|\mathbf{r} - \mathbf{R}_A|^{-1} + \sum_j^{\text{occ}}\{2J_j(\mathbf{r}) - K_j(\mathbf{r})\} - \mathbf{r}\cdot\mathbf{F} = h_0(\mathbf{r}) - \mathbf{r}\cdot\mathbf{F} \quad (10)$$

The matrix elements of $h(\mathbf{r})$ contain additional one-electron moment integrals, $\mathbf{M}_{pq} = \int \chi_p(\mathbf{r})\mathbf{r}\chi_q(\mathbf{r})d\mathbf{r}$; the latter integral can be fairly easily calculated at any level of approximation and has x – ($M^x_{pq} = \int \chi_p(\mathbf{r})x\chi_q(\mathbf{r})d\mathbf{r}$), y – ($M^y_{pq} = \int \chi_p(\mathbf{r})y\chi_q(\mathbf{r})d\mathbf{r}$), and z – ($M^z_{pq} = \int \chi_p(\mathbf{r})z\chi_q(\mathbf{r})d\mathbf{r}$) components. However, one has to realize that the self-consistent procedure applies to the solutions of $h(\mathbf{r})$. More specifically, the elements D_{rs} of the density matrix are now field-dependent quantities, $D_{rs}(\mathbf{F})$ weighting the two-electron integrals in the molecular matrix elements:

$$h_{pq} = \int \chi_p(\mathbf{r})h(\mathbf{r})\chi_q(\mathbf{r})d\mathbf{r} = T_{pq} - \sum_A Z_A V_{pq|A} - \mathbf{F}\cdot\mathbf{M}_{pq} + \sum_{r,s} D_{rs}(\mathbf{F})\{2(pq|rs) - (pr|qs)\} \quad (11)$$

The FF version of the coupled Hartree–Fock method provides acceptable and useful estimates of the polarizability components α_{ij}. This, because the FF approach takes into account, directly and in a self-consistent way, the orbitals relaxations in the presence of the perturbing external electric field. The components of the (hyper)polarizability tensors are obtained from derivatives of the field-dependent dipole moment with respect to the external electric field in the limit of zero field. In practice, the components α_{ij} are evaluated numerically by using the following approximation for differentiating the dipole moment components with respect to the field:

$$\alpha_i = \left\{\frac{\partial\langle\mu_i\rangle}{\phi F_i}\right\}_{\mathbf{F}=0} = \frac{1}{2F_i}[\mu_i(F_i) - \mu_i(-F_i)] \quad (12)$$

Large values of the field intensity $\mathbf{F}$ may be thought to be preferable in terms of numerical precision on α, which is proportional to $\Delta\mu/F$, where $\Delta\mu$ is an estimate of the numerical error on the dipole moment. The difference between the last two values of the dipole moment before convergence at the required level of accuracy may be taken as a rough estimate of $\Delta\mu$. However, higher values of $\mathbf{F}$ will increase the difference between the finite difference approximation of the di-

pole derivative and its actual value. In addition, at higher values of **F**, self-consistency is not easily reached, and generally the best value for **F** will be that just below numerical divergence threshold. The values of the electric field components actually used in the numerical procedure are equal to +0.001 and −0.001 au (1 au of electric field = 5.1423×10^{11} V m^{-1}). The values of polarizabilities reported in this paper are expressed in au (1 au of polarizability = 1.6488×10^{-41} C^2 m^2 J^{-1}).

Most calculations have been performed with the Gaussian 86 series of programs,[33] adapted for a FPS-164 and FPS-364 processors attached to an IBM 9377/90 computer. A code for the FF evaluation of electric polarizability has been added to the original Gaussian 86 software. The Fletcher–Powell procedure was used to minimize the forces on the nuclei and the standard threshold conditions of the Gaussian 86 program have been kept, i.e. 10^{-10} au for the two-electron integrals cutoff, 10^{-9} for the requested convergence on the density matrices, and 5.0×10^{-4} hartree bohr^{-1} as the minimum residual forces on the cartesian components.

V. Model Calculations

In these model calculations, our attention has been restricted to the linear response coefficients α_{ij} because, on the one hand, the first hyperpolarizability as such is of limited interest for the design of active main-chain polymers which are basically centrosymmetric, and, on the other hand, reliable calculations of the second hyperpolarizability are so far not possible for molecules of the complexity that is of interest in this paper. Fortunately, measured hyperpolarizabilities usually parallel the trends (enhancement or attenuation) observed for polarizability, and empirical models to relate hyperpolarizabilities to the linear polarizability have been proposed on the basis of these observations. Similarly, test calculations on conjugated chains indicate that these assumptions are reasonable.[34] Accordingly, we base the investigations reported in this chapter on the postulate that the variations obtained for the mean polarizability, $\langle\alpha\rangle = [\alpha_{xx} + \alpha_{yy} + \alpha_{zz}]/3$, will be indicative of the trends for the average second hyperpolarizability, $\langle\gamma\rangle = [\gamma_{xxxx} + \gamma_{yyyy} + \gamma_{zzzz} + 2\gamma_{xxyy} + 2\gamma_{xxzz} + 2\gamma_{yyzz}]/5$.

An important aspect of ab initio calculations is the choice of the basis set which describes the electron-distribution reorganization resulting from the external perturbation. It determines both the quality and the cost of the results.[35] Because of the size of the systems treated and the need for results obtained at the same level of accuracy for comparison purposes, the minimal STO-3G basis has been used for all the molecules considered, except in the case of silicon compounds considered in section V.A.5. In spite of its obvious limitations, the STO-3G basis predicts molecular structures reasonably well in the sense that errors on bond distances and angles remain fairly constant for a wide variety of molecular structures[36] and thus corresponds to the seeked conditions for a theoretical design of organic molecules and polymers for optoelectronics. It must be recalled that polarizability is quite sensitive to geometry and therefore it is preferable that all geometries be optimized at a common level of theory to avoid geometry effects in the predictions. Similarly, good qualitative estimates of the polarizability of conjugated hydrocarbons as well as structures including the common heteroatomic bondings have been noted with the STO-3G basis.[37] However, the components characterizing the direction perpendicular to the conjugation plane are systematically and grossly underestimated; this is true unless very extended basis sets are used. Thus, the predictions based on the STO-3G basis cannot be better than semiquantitative, but this is already acceptable for the immediate purpose of ranking molecules of similar composition and/or structures for a particular optoelectronic property.

As already pointed out, the design of active main-chain polymers for optoelectronics includes many aspects and questions into which insight from quantum chemistry calculations can be useful. Except for calibration purposes with known results, experimental or theoretical, isolated calculations are usually not very useful if not placed in the general context of the research. By providing a unified and logical research proposition, it is our purpose in this chapter to illustrate not only the variety of questions but also their dependence.[38] It is with this in mind that we have chosen illustrations from our ongoing research on finding the characteristics an active main-chain polymer should have to exhibit high electric response. The problems arise at different levels, each being the heading of a section in the sequel.

First, it is sensible that for exhibiting high electric response a polymer should be made out of already polarizable monomeric units. Experiment and theory agree on the fact that conjugated structures with electronic and structural "homogeneity" are usually best for large electric responses. However, it can be important for various reasons to alter this homogeneity by inserting heteroatomic functions in a given conjugated structure, and thus it is useful to predict the influence of these alterations on the overall response. Assessing the polarizability of monomeric units will be the subject of section V.A.

One of the interests in active main-chain polymers is the possibility to increase the delocalization of the π electrons and thus the electric response along the backbone by connecting conjugated units. However, as wel shall see, it is not necessarily true that connecting conjugated moieties will lead to enhanced response, even when structural ideality is assumed. This forms the subject of section V.B.

The organization at the molecular level is also important since sequences of conjugated units, sometimes assembled with great difficulties, do not distribute in an ordered way and the net response is reduced accordingly. Quantum chemistry can investigate the question of forcing the order, e.g. with hydrogen bonds, while not overly spoiling the net electric response. Results along these lines are reported in section V.C.

Finally, doping can force π-electron structure to relax in such a way that enhanced electric responses result. This constitutes the subject of the last section, V.D.

A. Monomers

In addition to problems concerning the synthesis, stability, etc., there arises the question of assessing the intrinsic merits of the repeating units of conjugated polymers. This evaluation cannot be isolated from the other aspects of the problem. One may decide to favor

TABLE I. Longitudinal Polarizability, α_{zz}, of Four Conjugated Molecules Containing Six π Electrons[a]

molecule	α_{zz}	α_{zz}/l_π	α_{zz}/V
benzene (1)	45.26	30.72	0.083
hexatriene (2)	104.13	30.55	0.172
vinylacetylene (3)	44.65	24.08	0.113
butatriene (4)	74.23	36.40	0.189

[a] The polarizability is expressed in atomic units; l_π and V are measures, respectively, of the conjugated pathway (in bohr) and of the molecular volume (in bohr^3).

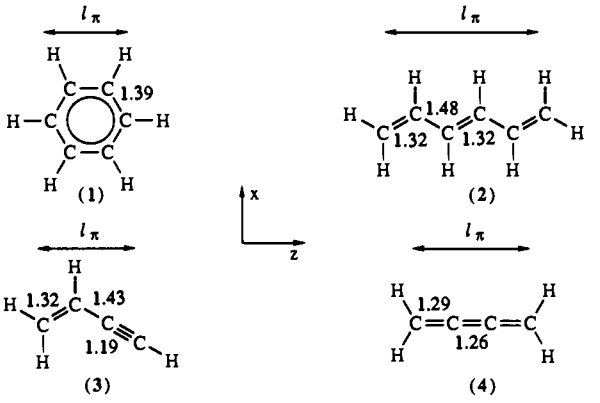

Figure 1. Schematic representation of molecules 1–4 and relevant distances (in Å).

the organization at the molecular level (order, packing, etc.), or pay attention to the stability of the resulting material, or both. This often imposes to compromise between the wish of having very effective repeating units (e.g. highly polarizable units) and the need to meet other constraints conflicting with the best available units. For example, contrary to normal intuition, the polarizability of conjugated structures does not always scale linearly with the number of π electrons they contain. Quantum chemistry calculations can provide relatively fast and economic ways of performing reliable assessment of various molecular structures. This is illustrated in the paragraphs V.A.1–V.A.5.

1. Molecules Containing the Same Number of π Electrons: A Comparison

The longitudinal polarizability α_{zz} of four molecules, benzene (1), *trans*-1,3,5-hexatriene (2), vinylacetylene (3), and butatriene (4),[38] all containing six π electrons, are compared in Table I.

The calculations have been performed at the STO-3G level and all geometrical parameters have been optimized at that level of the theory. The corresponding structures are represented in Figure 1.

The molecular planes coincide with the x,z plane, the z axis being along the direction of maximal extension of the molecules and the y axis perpendicular to the molecular plane. The total longitudinal polarizability α_{zz} is not the best quantity to consider when comparing molecules for their electric response, but instead the polarizability divided by the scale of the molecule since what is important in a material is the density of active species. In the case of chain systems, the length could be appropriate to scale the longitudinal polarizability. As indicated in Figure 1, l_π is the vector distance (in bohr) between the most distant carbons; it provides a qualitative (admittedly arbitrary) measure of the molecules extension. A more appropriate quantity, however, is the molecular volume, V, because the molecular anisotropy is not always as important as in butatriene, for example. V is the volume enclosed in the van der Waals spheres centered on each atom of the molecules; the volumes due to sphere overlaps are subtracted.

Values in Table I show important differences in the polarizability values of the structures 1–4 in spite of the fact that they contain the same number of π electrons. The first point is that vinylacetylene (3) and benzene (1) are the less polarizable of the four molecules, in absolute value and relative to both measures of their dimension, l_π and V. Hexatriene (2) is quite polarizable, which points to a more effective delocalization of the six π electrons along the molecular backbone. Vinylacetylene (3), the template repeating unit found in polydiacetylenes, is much less polarizable than hexatriene. This difference is due to a strong confinement of the four π electrons corresponding to the C≡C bond, which leads to an overall less effective delocalization. Finally, butatriene (4), a cumulenic structure, shows an appreciable polarizability value. This analysis stresses the significant dependence of the polarizability upon molecular structure. In particular, the extension of the conjugated backbone over which the π electrons distribute is important to know. In absence of data on the molecular structure, quantum chemistry can supplement the missing information with quite acceptable confidence.[36] Note that benzene (1), which has good chemical stability and tendency to induce local order due to its planar structure, is often incorporated in polymer backbones for these two reasons. Unfortunately the polarizability of isolated benzene (1) is not as much appealing.

If α_{zz} is scaled according to the dimension of the molecules, either by the length l_π or the volume V, some reordering occurs: butatriene (4) turns out to be better than hexatriene (2). Both hexatriene (2) and butatriene (4) are intrinsically more polarizable than vinylacetylene (3). As already pointed out, vinylacetylene (3) is the basic repeating unit of polyacetylene which is, to our knowledge, the active main-chain polymer having the highest measured third-order nonlinear susceptibility $\chi^{(3)}$. From these calculations it appears that higher responses should be possible with new polymers based on other repeating units, provided the other conditions on stability, molecular organization, transparency, light scattering, etc. are met.

Comparison of the molecular structures in Figure 1 with their polarizability suggests that the more homogeneous the molecular structure and thus the electron distribution and the more polarizable is the system. As will be seen in the sequel, this seems to be quite general and could be used as a simple and convenient rule in the design of molecules for optoelectronics. However, direct calculations are required to obtain more quantitative information on the importance of the polarizability gain with respect to geometry changes.

2. Dependence of the Longitudinal Polarizability on the Molecular Structure[37b,39]

As already mentioned, the longitudinal electric polarizability depends on the molecular structure. In the case of polydiacetylene crystals,[40] large structural variations can actually be produced, e.g., by application of

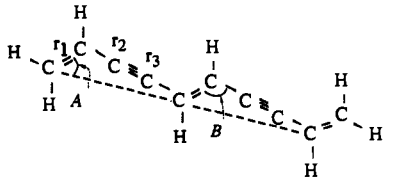

Figure 2. Structure of the 1,5,9-decatriene-3,7-diyne molecule (5).

TABLE II. Geometries and STO-3G-Calculated Longitudinal Electric Polarizability, α_{zz}, of 1,5,9-Decatriene-3,7-diyne (5) with Different Geometrical Parameters To Model the Basic Repeat Unit of PDA, PTS, TCDU and PBT

oligomer	r_1, Å	r_2, Å	r_3, Å	A, deg	B, deg	α_{zz}, au
PDA[a]	1.31	1.43	1.19	43.2	123.9	183.7
PTS[b]	1.36	1.43	1.21	44.5	121.9	205.5
TCDU[c]	1.42	1.38	1.24	39.3	127.7	302.7
PBT[a]	1.44	1.32	1.25	41.9	123.7	412.4

[a] Optimized geometry taken from ref 41. [b,c] Experimental Geometries taken from ref 40b,c, respectively.

hydrostatic pressure, mechanical deformation, or stresses induced by side groups. Thus, it is interesting to investigate in a systematic way the importance of structural modifications on α_{zz} for various model oligomers of polydiacetylenes. Here, the active part of their backbones is modeled by various geometries of the 1,5,9-decatriene-3,7-diyne (5) molecule represented in Figure 2. These geometries will be denoted under the names PDA, PTS, TCDU, and PBT, which, in the case of PTS and TCDU, refer to the existing polymers, but where the actual side groups have been replaced by hydrogen atoms. The geometrical parameters and the longitudinal polarizability are given in Table II. To the names PDA and PBT correspond the hypothetical structures of an ideal polydiacetylene and an ideal polybutatriene; their structures have been obtained by geometry optimization of the corresponding infinite model chain.[41]

PTS and TCDU polydiacetylenes exhibit different bond lengths in the polymer backbone as seen in Table II; the first one adopts an acetylenic-type structure whereas the second one is closer to a butatrienic configuration. This difference in the geometry induces significant variations in the longitudinal polarizability values as it can be observed in Table II, where the longitudinal polarizability is shown to double from PDA to PBT.

Scaling rules,[42] which relate the linear α and the second hyperpolarizability γ_{ijkl}, suggest that α_{ij} scales with the length of conjugation l_π to the third power, whereas γ_{ijkl} scales to the fifth power of that length. Thus, a modest increase in α_{ij} can become significant when it comes to γ_{ijkl}, and controlled geometry alterations toward higher structural homogeneity to favor the π-electron delocalization may represent an interesting way to raise the electric response of organic systems. This can be done in various ways; an attempt along these lines forms the subject of the next illustration.

3. Structure and Polarizability of Acetylenic Analogues of Carbocyanines[43]

As we have just seen, substantial electronic polarizations are generally obtained in systems with valence electrons highly delocalized over large distances as noted in conjugated oligomers. Carbocyanines, H_2N-$(CH{=}CH)_nCH{=}N^+H_2$, are characterized by a highly delocalized conjugated pathway evidenced both by a low degree of alternation between double and single bonds[44] and high polarizability of their backbones.[45] This idea was already developed in the lat 1940s by Kuhn.[46] It was his pioneering contribution to relate the nature of the first π-π^* transition to the concept of bond alternation in conjugated chains particularly in the even-atom polyene and in the odd-atom polymethine chains. Indeed, Kuhn showed that in the series of polymethine dyes, the bond lengths between all the carbon atoms are equal due to a resonance balance between equivalent extreme forms:

$$>N{-}(CH{=}CH)_n{-}CH{=}N^+< \leftrightarrow >N^+{=}CH{-}(CH{=}CH)_n{-}N<$$

All carbon–carbon bonds in the skeleton have 50% double bond character. This fact was later confirmed by X-ray diffraction studies. A simple free-electron (FE) model calculation shows that there is no energy gap between the valence and conduction bands and the limit of the first UV–visible transition for an infinite chain is zero. In contrast, when the same approach is used in the case of polyenes (polyacetylenes), a much poorer agreement with experiment is obtained. In order to reproduce the experimental data, Kuhn had to include a sinusoidal perturbative potential so that the electronic distribution corresponds to alternating single and double bonds. In this case, the extrapolation of the UV spectrum tends to a nonzero energy gap for the infinite chain. This question has been investigated in more detail[47] by plotting the FE transition energies of the series of oligomers $>(CH{=}CH)_n<$ (for n = 2,3, ...6) and $>N{-}CH{=}CH)_n{-}CH{=}N^+$ (for n = 1, 2, ...5) as compared to the experimental values taking into account the box length as adjustable parameters. In the polymethine series, the regression line has its y intercept at the origin of the axis. As expected, it corresponds to a zero energy gap, i.e., to a metallic character. In the polyene case, however, the y intercept is of the order of 1.8 eV, a value in close agreement with the experimental energy gap of polymeric polyacetylene. This discussion is of crucial importance in the present discussion, since in the Unsöld approximation polarizabilities are directly related to first electronic transitions. In this way, carbocyanine-based polymers should be significantly more polarizable than polyacetylenes. The question of bond alternation is thus quantitatively illustrated in Figure 3, where the relevant geometrical parameters (bond distances and bond angles calculated at the STO-3G level) are given for a series of four model carbocyanines, noted **6**–**9** of increasing length (n = 2, 3, 5, and 7).

Note that bond alternation is quickly restored as the carbocyanine chain length increases. The alternation degree of carbocyanines is classically formalized in terms of specific symmetric resonance structures, which are chemically induced through the interplay of the $-NR_1R_2$ ($=N^+R_1R_2$) and ($-NR_3R_4$) $=N^+R_3R_4$ end groups; the corresponding resonant structures are shown in Figure 4a.

Since the electronic polarization, in addition to the delocalization length, directly depends upon the number of active valence electrons per repeat unit, we address

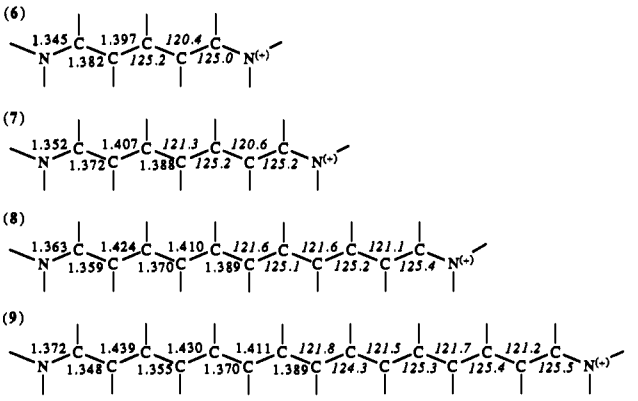

Figure 3. Bond lengths (in Å) and bond angles (in degrees) of four carbocyanines of increasing length $H_2N(CH{=}CH)_nCH{=}N^+H_2$ (n = 2, 3, 5, and 7). The geometries have been optimized at the STO-3G level.

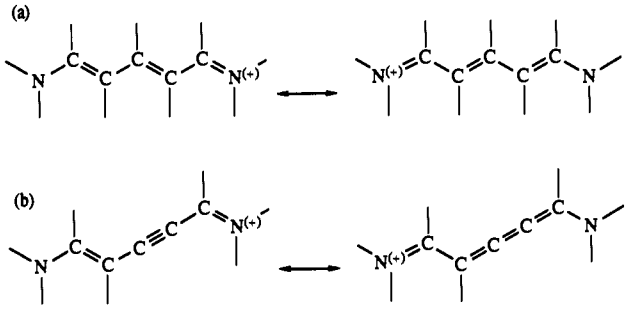

Figure 4. Resonance structures invoked for (a) classical carbocyanines and (b) their acetylenic analogues.

the possibility of chemically deconfining π-electron-rich moieties such as the —C≡C— triple bond to increase the number of electrons participating to the electronic response. The hope is that by inserting a triple bond in a carbocyanine backbone, the —C≡C— distance will increase and lead to enhanced polarizability; the resonance forms for acetylenic carbocyanines are shown in Figure 4b.

To our knowledge, the first synthesis of an acetylenic cyanine has been made by Mee et al.[48] They noted an hypsochromic shift of the first optical transition as compared to those of the carbocyanine analogues (i.e., containing the same number of carbon atoms). They explained this shift on the basis of the asymmetric electron distribution of the acetylenic cyanines. This can also be related to the resonance structures shown in Figure 4b, which are not equivalent as opposed to the carbocyanine case (Figure 4a). In Figure 4b, one of the resonance structure is reminiscent of the monomer unit of polydiacetylene, while the second is typical of the butatrienic form. Butatriene belongs to the family of cumulenes which seem to be the most polarizable of the conjugated chains investigated so far.[49] It is thus interesting to determine which of these two limiting forms is dominant in the representation of the actual structure. A series of five molecules, denoted **10**–**14** and shown in Figure 5, has been considered. Molecule **10** is the simplest of the acetylenic cyanines; molecules **11**–**13** are isoelectronic to **10** and differ only by the nature of their chain ends. Note that for a sake of clarity, molecule **14** has been taken as identical with molecule **6**. The general formula is $R_1(CH{=}CH)C{\equiv}CCH{=}R_2$. For comparison purposes, the results for carbocyanine (**14**, $H_2NCH{=}CHCH{=}CHCH{=}N^+H_2$)

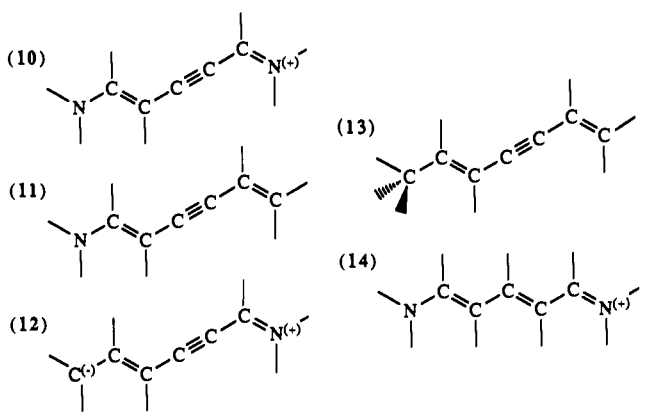

Figure 5. Molecular structure of the series of related molecules **10**–**14**.

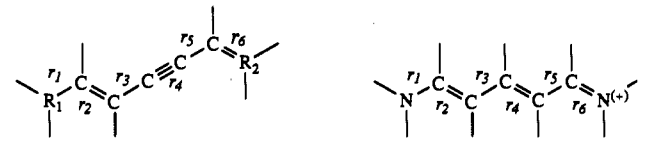

Figure 6. Numbering system used to denote the bonds in molecules **10**–**14**.

TABLE III. STO-3G-Optimized Bond Lengths (in Å) for Five Molecules (10–14)

	R_1	R_2	r_1	r_2	r_3	r_4	r_5	r_6
10	NH_2	NH_2^+	1.351	1.373	1.389	1.208	1.371	1.335
exptl[a]			1.370	1.386	1.376	1.212	1.394	1.356
11	NH_2	CH_2	1.395	1.329	1.444	1.178	1.451	1.316
12	CH_2	NH_2	1.315	1.483	1.309	1.246	1.308	1.400
13	CH_3	CH_2	1.519	1.319	1.452	1.177	1.453	1.316
14 = 6	NH_2	NH_2^+	1.345	1.382	1.397	1.397	1.382	1.345

[a] Experimental data have been added in the case of molecule **10**.

have been added to the series. Both the equilibrium geometry and polarizability have been computed for these molecules by using the same conditions as described above. The optimized geometries have been used as input for static dipole polarizability calculations.

Equilibrium geometry parameters are listed in Table III according to the convention shown in Figure 6. The results show that the carbon framework, (CH=CH)-C≡CCH=, common to all structures, is quite sensitive to the nature of the chain ends. Note first the satisfactory agreement between experimental and theoretical predictions for **10**. Molecule **10** has a structure intermediate between acetylenic and butatrienic forms. Only r_4 is substantially shorter (1.208 Å) than the other CC bonds in the molecule; a typical —C≡C— bond length at the STO-3G level is 1.170 Å.[36] This indicates a net increase of the —C≡C— bond length due to its incorporation in a cyanine type structure. Molecules **11** and **13** exhibit values typical of an acetylenic bond length and, from our previous experience,[37b,39] it is anticipated that their electric polarizability will be smaller than that for molecule **10**. Molecule **13** has a clear butatrienic configuration which originates from the constraining effect of the $=CH_2$ group on the left side of the structure.

Absolute value of the average polarizability for molecules **10**–**14** are given in Table IV. However, to make a fair comparison between the five systems, it is more appropriate to consider the average polarizability divided by the total number of electrons in each mol-

TABLE IV. Average Polarizability, $\langle\alpha\rangle$ (in au), and Average Polarizability Divided by the Number of Electrons, n_e, in the Molecule $(\alpha/n_e)^a$

	$\langle\alpha\rangle$	n_e	$\langle\alpha\rangle/n_e$
10	68.25	50	1.36
11	46.36	50	0.93
12	63.67	50	1.27
13	46.07	50	0.92
14 = 6	73.30	52	1.41

ecule. The largest polarizability is obtained for carbocyanine (14), followed by acetylenic cyanine 10 which has a geometrical structure intermediate between the alternating acetylenic structure and the more regular butatrienic form. Then comes molecule 12, which includes a butatrienic structure in its skeleton. Finally molecules 11 and 13 have the smallest values of polarizability in good agreement with the fact that the —C≡C— triple bond has not been affected.

Thus, as hoped at the beginning of this study, the acetylenic cyanine exhibits a net polarizability enhancement over isoelectronic molecules 11 and 13 for which the r_4 distance is basically a —C≡C— triple bond in which the four π electrons remain strongly confined. The most polarizable system is still the classical carbocyanine (14). Also interesting to note is the fact that even though molecule 12 incorporates a butatrienic structure, it is still less polarizable than 10. This is due to the fact that delocalization in 14 takes place over the entire molecule, while in 12 the electronic delocalization is interrupted at r_2 (1.483 Å = the longest C–C bond distance found in the molecules 10–14).

The largest polarizability is noted for the classical carbocyanine (14), which also has the maximum equalization of bond distances and thus the best chances for electronic delocalization of the structures considered in this work. Acetylenic analogue 10, which has a structure intermediate between the vinylacetylene and butatriene forms, has the next largest polarizability. Compound 12, which exhibits a butatriene-like structure known to be a highly polarizable fragment, has nonetheless an average polarizability smaller than those of 14 and 10. This is because of the large r_2 distance which, as pointed out in the theoretical analysis by Flytzanis,[42] disrupts the actual delocalization and limits its extent to a smaller portion of the molecular framework. The results on the triply bonded moiety (—C≡C—) are somewhat deceptive, but other fragments could be more suitable.

4. Peptide Groups in Conjugated Hydrocarbon Chains[38]

Another example of altering the structural homogeneity of conjugated hydrocarbon chains is provided by the incorporation of a peptide or amide bond, –NHCO–, into a butadiene backbone. As shall be discussed in section V.C, peptide-like bonds could be used as chemical tools to force the organization of active molecules and/or polymers in the bulk. Therefore it is interesting to estimate their influence on the resulting polarizability of a conjugated system that incorporates such heteroatomic groups. In Figure 7 are shown two molecules, *N*-vinylacrylamide (15) and *N*-butadienylformamide (16), containing two C=C double bonds and an amide group. In the first system (15), the C=C double bonds are separated by the –NHCO– group, while in 16 these

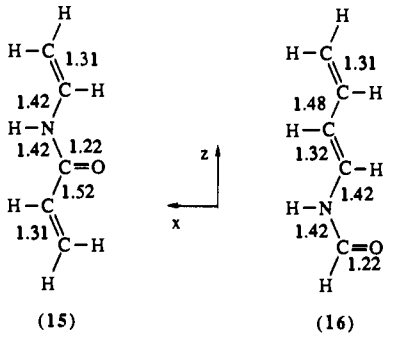

(15) (16)

Figure 7. Relevant bond distances (in Å) of *N*-vinylacrylamide (15) and *N*-butadienylformamide (16).

TABLE V. Longitudinal Polarizability, α_{zz}, Average Polarizability, $\langle\alpha\rangle$ (in au), and l_π, the Delocalization Length (in Å), for Molecules 2, 15, and 16

molecule	α_{zz}	$\langle\alpha\rangle$	l_π
N-vinylacrylamide (15)	64.29	36.26	6.04
N-butadienylformamide (16)	76.36	41.25	6.15
trans-1,3,5-hexatriene (2)	104.13	43.93	6.13

C=C bonds are directly connected. This procedure of comparison has been chosen to eliminate, as much as possible, the deficiencies due to the limited basis used. In Table V are given the longitudinal polarizability, α_{zz}; the average polarizability, $\langle\alpha\rangle$; and the delocalization distance, l_π. Polarizability and fully optimized geometries for molecules constrained to remain planar have been obtained with the STO-3G basis set. The relevant bond distances are given in Figure 7. The corresponding results for the *trans*-1,3,5-hexatriene for comparison have been added in Table V.

On the basis of the longitudinal and the average polarizability values given in Table V, the amide group —NHCO—, even with its four π electrons, is less polarizable than a C=C double bond with only two π electrons. In a peptide group the C–N bond has some degree of double bond character resulting from the delocalization of the nitrogen lone pair into the carbonyl group; the calculated C–N bond distance is 1.42 Å in *N*-vinylacrylamide (15) and *N*-butadienylformamide (16). This bond length is intermediate between a true C=N bond, 1.27 Å in $H_2C{=}NH$, and a single C—N bond, 1.48 Å in $H_3C{-}NH_2$, both calculated at the STO-3G level.[31] A similar delocalization is not observed for the C–C bond adjacent to the carbonyl group, in that case the bond distance is 1.52 Å, which is typical for a single C–C bond. Thus, in *N*-vinylacrylamide (15) the C=C double bond is in a way isolated from the rest of the conjugated framework of the molecule. This is not the case in *N*-butadienylformamide (16), where the carbonyl group is located at the end of the molecule. Even in this case and in spite of the four π-electrons brought by the peptide group, the overall polarizability is not as large as in *trans*-1,3,5-hexatriene (2). Notice also that *N*-butadienylformamide (16) is slightly more stable than *N*-vinylacrylamide (15); at the STO-3G level the difference of stability is of the order of 1 kcal mol^{-1}. Thus peptide bonds, when incorporated in a conjugated hydrocarbon chain of the polyene type, disrupt significantly the conjugation and should not be used unless they can serve other important purposes such as inducing local order. It must be kept in mind however that when located at the end of a molecule, peptide groups do not spoil the polarizability as much as when

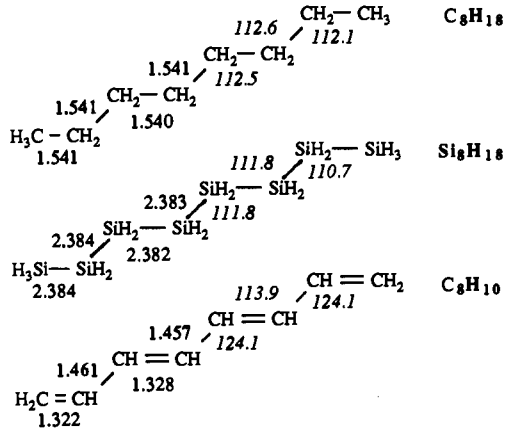

Figure 8. Relevant bond distances (in Å) of alkane, polyene, and silane chains.

they are incorporated in the conjugated backbone. Therefore, they still could be used as terminal groups to enhance the organization of the active species in the bulk.

5. Alkane, Polyene, and Silane Chains: A Comparison[50]

Silicon-based polymers, especially polysilanes, have recently been the subject of an increasing number of studies for their electronic properties[51] in general and, in particular, for their nonlinear optical properties.[52] Already in 1986, Bigelow and McGrane obtained from MNDO calculations that the ground-state electronic distribution of the saturated silane oligomers are considerably more polarizable than a fully conjugated polyene backbone of comparable length.[53] In this subsection, we compare the computed equilibrium geometry and electric polarizability of polyethylene, polyacetylene, and polysilane model compounds, respectively referred to as $H(CH_2)_{2x}H$, $H(CH)_{2x}H$, and $H(SiH_2)_{2x}H$, with x ranging from 1 to 4. Full geometry optimizations have been carried out with the split valence 3-21G basis set[54] on the model systems in the D_{2h} symmetry. The D_{2h} symmetry corresponds to the planar zigzag conformation that has been shown to be more stable than the helical gauche form in a recent polymer band structure calculation on polysilane.[55]

The optimized geometries have been used as input for static dipole polarizability calculations with the 3-21G basis set. This 3-21G basis provides a reasonable compromise between cost and reliability of polarizability estimates.[56] The resulting optimized geometrical parameters of interest for C_8H_{18} (**20**), C_8H_{10} (**24**), and Si_8H_{18} (**28**) results are displayed in Figure 8. The hydrocarbon compounds do not need special attention since they have already been discussed at length for the conjugated systems[57] and for the saturated ones.[36] In the case of the silicon oligomers, our results are in good agreement with the bond lengths and angles reported by Teramae[58] for the first terms of the $H(SiH_2)_{2x}H$ series. With respect to the electrical polarizabilities to be discussed, it must be pointed out that for the same stoichiometry, the chains containing silicon atoms are roughly 1.5 times longer than their corresponding hydrocarbon analogues. This is important because it is known from the work by Flytzanis[42] that the conjugation length is a major condition to have highly polarizable structures.

TABLE VI. Molecular Volume, V (in bohr^3), Average 3-21G Polarizability, $\langle\alpha\rangle$, Longitudinal 3-21G Polarizability, α_{zz} (in au), and Longitudinal 3-21G Polarizability per Volume, $\langle\alpha\rangle V^{-1}$, for the Series of Oligomers Considered in This Paper[a]

oligomer	V	α_{zz}	$\langle\alpha\rangle$	$100 \times (\langle\alpha\rangle V^{-1})$
C_2H_6 (17)	318.7	22.20	21.32	6.69
C_4H_{10} (18)	507.2	45.47	40.70	8.02
C_6H_{14} (19)	739.3	71.30	60.49	8.18
C_8H_{18} (20)	956.3	98.24	80.56	8.42
$K = 21.97$, $a = 1.07$				
C_2H_4 (21)	251.7	30.73	18.34	7.29
C_4H_6 (22)	429.3	73.55	40.11	9.34
C_6H_8 (23)	613.1	136.69	68.53	11.18
C_8H_{10} (24)	782.2	218.20	103.02	13.17
$K = 24.53$, $a = 1.57$				
Si_2H_6 (25)	529.5	59.97	48.36	9.13
Si_4H_{10} (26)	959.2	144.08	105.36	10.98
Si_6H_{14} (27)	1400.7	253.04	168.77	12.05
Si_8H_{16} (28)	1830.7	374.05	235.84	12.88
$K = 55.70$, $a = 1.38$				

[a] Parameters K and a in the relationship $\alpha_{//} = Kx^a$ between the longitudinal polarizability and the number (x) of carbon or silicon atom pairs in the chains.

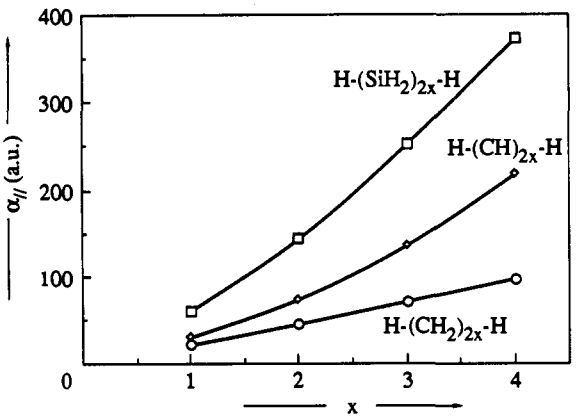

Figure 9. Trends in polarizability in the series of alkane, polyene, and silane chains.

The longitudinal polarizability, α_{zz} (longitudinal means parallel to the chain direction), the average polarizability, $\langle\alpha\rangle$, and the molecular volume, V, are presented in Table VI for the series of molecules $H(CH_2)_{2x}H$, $H(CH)_{2x}H$, and $H(SiH_2)_{2x}H$ with x ranging from 1 to 4.

Comparison of the evolution of the polarizability between the sets of compounds versus the chain length indicates that the largest increase in the longitudinal polarizability (α_{zz}) and $\langle\alpha\rangle$ is found for the polysilane series in Figure 9. Our results confirm the previous predictions by Bigelow and MacGrane[53] on the larger polarizabilities of the polysilane chains compared to the fully conjugated polyene framework of comparable length. Note, however, that the exponent a, 1.38 and 1.57, respectively, for $H(SiH_2)_{2x}H$ and $H(CH)_{2x}H$ (see Table VI), in the mathematical fit $\alpha_{zz} = Kx^a$ reveals that long polyene chains will ultimately be more polarizable than the saturated silane oligomers. Nevertheless, these exponent values are sufficiently close that it will take very long polyene chains before they exhibit polarizabilities similar to their silane analogues (in absence of additional effects such as the saturation of the polarizability, a straightforward extrapolation of the data in

Table VI shows that the crossing point should roughly occur for approximately 75 pairs of carbon or silicon atoms). These results support the often used terminology of "σ conjugation" for polysilanes.[55,59]

Silicon polymers appear to be very promising compounds for optoelectronics and further quantum chemistry studies could provide additional information on their potentialities. Several questions regarding their chemical stability, molecular structure, chain length, and effects of incorporating heteroatoms in silicon-based chains or incorporating silicon moieties in conjugated hydrocarbon chains should be addressed.

This series of examples on assessing the delocalization of electrons in various conjugated frameworks, π and σ, is far from being exhaustive, but it should convey some idea on how quantum chemistry calculations can be used in the context of the design of highly polarizable systems. In the next section, we consider chain length increase as a way to enhance the polarizability.

B. Dependence of the Polarizability on the Chain Length

We have already noted that it is important to scale the polarizability values according to the length of the conjugated framework l_π or some other quantity, such as the molecular volume, V, to have a suitable measure of the intrinsic polarizability of a given conjugated system. In several cases, connecting conjugated units together leads to a net polarizability that is more than additive in the constituent contributions. For example, in polydiacetylenes the one-dimensional delocalization that results from the polymerization of diacetylene molecules produces a dramatic enhancement of the optical nonlinearities of these compounds. The TCDU polymer $[-CR{=}CRC{\equiv}C-]_x$, where R is $(CH_2)_4OCONHPh$, shows a response of 6×10^2 times that of the TCDU monomer.[7] Since large electric response is one of the main targets in the design of conjugated organic polymers for optoelectronics, this other way of enhancing the polarizability is certainly worth considering but with due attention to other requirements. It can be anticipated that not all units are equally appropriate for polarizability enhancement, and furthermore, one might be willing to mix units of different kinds. Therefore, model calculations carried out to assess the polarizability of various arrangements of units connected in a chain as a function of the chain length are certainly useful to define the most suitable choice out of a set of different possibilities.

The size-dependence of the electronic polarizability of conjugated systems has been studied first for metallic polyene (polyacetylene) chains within the framework of the free-electron and Hückel models; they predict a dependence of longitudinal polarizability α_{zz} proportional to l_π^3. According to these findings, the longitudinal polarizability should grow as the third power of the chain length and thus diverge in the limit of an infinite chain. On the one-hand, free-electron and Hückel theories do not take into account Coulombic interactions explicitly, and on the other hand, structural reorganizations in the chain cannot be ignored as the size increases. Bond alternation influence on the longitudinal polarizability of polyenes containing increasing number of carbon atoms has been investigated at the ab initio level. The quantity actually followed

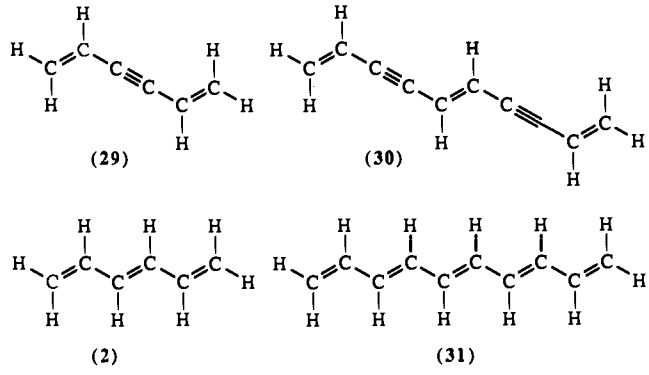

Figure 10. Schematic representation of 1,5-hexadiene-3-yne (**29**), 1,5,9-decatriene-3,7-diyne (**30**), *trans*-1,3,5-hexatriene (**2**), and *trans*-1,3,5,7,9-decapentaene (**31**) molecules.

TABLE VII. STO-3G Longitudinal Polarizability, α_{zz}, Average Polarizability, $\langle\alpha\rangle$ (in au), and l_π, the Delocalization Length (in Å), for Molecules 29, 30, 2, and 31

molecule	α_{zz}	$\langle\alpha\rangle$	l_π
1,5-hexadiene-3-yne (**29**)	44.65		
1,5,9-decatriene-3,7-diyne (**30**)	85.28		
trans-1,3,5-hexatriene (**2**)	104.13	43.93	6.13
trans-1,3,5,7-decapentaene (**31**)	217.25		

is the polarizability per vinylic moiety, α_{zz}/n. α_{zz}/n increases with the number of double bonds, but eventually saturates, indicating that a regime of linear increase has been reached. Also seen is the fact that the value at which α_{zz}/n levels off and the number of double bonds at which the linear regime prevails is strongly related to the degree of alternation measured as the difference between the lengths of the single and double carbon–carbon bonds. Note, however, that this dependence is not trivial and it is quite unlikely that the simple reference to bond alternation will be applicable to more complex systems. Even if this would be the case, one must still know from the start the geometrical parameters connecting the units and the possible structural relaxations in the units due to these connections. Here again, quantum chemistry calculations can provide useful quantitative support as to these structural changes and their incidence on the polarizability. To illustrate the above mentioned discussion, two cases concerning the influence of the oligomerization (connecting units) on the resulting polarizability are described.

1. Vinylacetylene and Polyene Chains[38]

In this first example, the influence of oligomerization on the longitudinal polarizability is examined by comparing 1,5-hexadiene-3-yne (**29**) and 1,5,9-decatriene-3,7-diyne (**30**), on the one hand, and *trans*-1,3,5-hexatriene (**2**) and *trans*-1,3,5,7,9-decapentaene (**31**), on the other hand. These molecules are schematically represented in Figure 10, the corresponding STO-3G values of the longitudinal polarizability, α_{zz}, and average polarizability, $\langle\alpha\rangle$, are reported in Table VII.

Going from 1,5-hexadiene-3-yne (**29**) to 1,5,9-decatriene-3,7-diyne (**30**) means adding 10 more π electrons with the $-C{\equiv}CCH{=}CHC{\equiv}C-$ moiety inserted between two vinylic groups, while going from *trans*-1,3,5-hexatriene (**2**) to *trans*-1,3,5,7,9-decapentaene (**31**) amounts to incorporate three C=C double bonds carrying a total of six π electrons between the two vinylic groups. The net gain in polarizability is more sub-

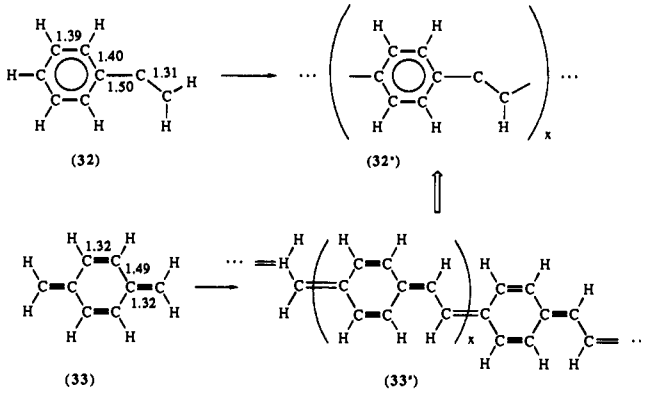

Figure 11. Schematic representation of 3,6-dimethylene-1,4-cyclohexadiene (**33**) and phenylethylene (**32**) molecules and of their polymerization schemes (**33'** and **32'**).

TABLE VIII. STO-3G Longitudinal Polarizability, α_{zz}, Average Polarizability, $\langle\alpha\rangle$ (in au), and l_π, the Delocalization Length (in Å), for Molecules 32 and 33

molecule	α_{zz}	$\langle\alpha\rangle$	l_π
phenylethylene (**32**)	76.39	47.53	4.94
3,6-dimethylene-1,4-cyclohexadiene (**33**)	125.41	55.81	5.45

stantial with the polyenic backbone, because of a more efficient delocalization of the π electrons in this geometrical framework. As already seen in the case of the acetylenic analogues of carbocyanines, section V.A.3, triple bonds, notwithstanding the fact that they are π-electron richer than double bonds, have their electrons more confined between the nuclear centers of the bond and form less polarizable structures.

2. Chains of Phenylethylene and 3,6-Dimethylene-1,4-cyclohexadiene[38]

In this second example, we speculate about the interest of having chains formed by the repetition of 3,6-dimethylene-1,4-cyclohexadiene (**33**) units compared to chains made out of phenylethylene (**32**) units. The molecules are represented in Figure 11 and the corresponding STO-3G values of the longitudinal polarizability, α_{zz}, and average polarizability, $\langle\alpha\rangle$, are reported in Table VIII.

In spite of its delocalized nature benzene disrupts the conjugation and thus, as seen in Table VIII, tends to spoil the overall polarizability of a conjugated system in which it is inserted. This can be related to its aromatic character. A possible way to weaken the aromatic character while retaining the overall geometry of benzene is to switch to a quinoidic structure as in **33**, where the Lewis structure points to delocalization channels favorable for enhanced polarizability. This is confirmed by the polarizability values given in Table VIII, where the value α_{zz} for **33** is 1.6 times larger than that of phenylethylene (**32**). Owing to the advantages of connecting conjugated moieties having substantial enhancements in the longitudinal polarizability (α_{zz}), it would a priori be nice to obtain polymer (**33'**) based on such repeating units.

Quinoidic structures are not easy to handle and, in particular, forming a polymer of such units is a difficult synthesis problem. Therefore it is useful to know beforehand the extent of the resulting polarizability enhancement to decide whether or not attempting the preparation of such type of compound. Irrespective of the advantages polymer **33'** would have for polarizability in the ideal structure (i.e. regular and planar) shown in Figure 11, for stability reasons polymer **33'** will isomerize into poly(*p*-phenylenevinylene) (**32'**). This can be guessed from total energies calculated at the ab initio level on the repeat units. Computed at the 6-31G level, the stability difference between 3,6-dimethylene-1,4-cyclohexadiene (**33**) and phenylethylene (**32**) is 25 kcal mol^{-1}, the latter being the more stable molecule.

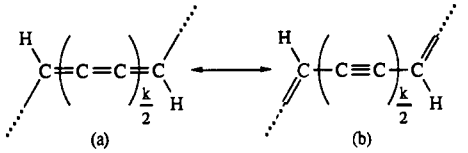

Figure 12. Two resonance forms of cumulene chains.

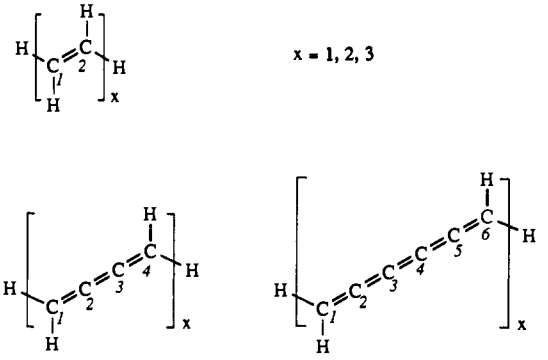

Figure 13. Schematic representation of the H[—HC_1=C_2H—]$_x$H, H[—HC_1=C_2=C_3=C_4H—]$_x$H and H[—HC_1=C_2=C_3=C_4=C_5=C_6H—]$_x$H oligomers, x = 1, 2, and 3.

3. Oligomers of Cumulenes[49b]

As we have seen in section V.B.1, butatriene (**4**) is intrinsically more polarizable than *trans*-1,3,5-hexatriene (**2**). Butatriene is part of the cumulene family which can be divided into two classes. The first class, $R_1R_2C[{=}C{=}]_kCR_3R_4$, is characterized by an even number, k, of directly connected carbons, while the second class contains those molecules for which k is an odd number. Here we will only be concerned with the first class, i.e. molecules for which k is even. When such molecules are linked together to form oligomers, the two resonant structures shown in Figure 12 are worth considering to understand the structural changes that will take place as the chain length increases. Form b is more stable than form a and it can be expected that in the limit of large k values, the actual structure will essentially correspond to form b. Therefore, in the same line as in the previous sections, it is interesting to know when form b becomes predominant over form a, which eventually means that the intrinsic polarizability starts to level off.

Full geometry optimization for all angles and distances of the molecules shown in Figure 13 (forced to adopt a fully stretched configuration) has been carried out at the STO-3G level. Only the C=C and C—C bond distances are of interest to us here; they are listed in Table IX. In the dimers, the repeat units are related through inversion symmetry, and therefore only the geometrical parameters corresponding to one units are listed. In the case of the trimers, the listed structural data have been limited to the values corresponding to the central units since they are more characteristic of

TABLE IX. STO-3G Carbon–Carbon Distances (in Å) for Three Series of Cumulenes[a] with Even Numbers of Directly Connected Carbons

H[—HC$_1$=C$_2$H—]$_x$H

	x	$r_{C_1=C_2}$	r_{C-C}
ethene	1	1.306	
butadiene	2	1.313	1.489
hexatriene	3	1.322	1.485

H[—HC$_1$=C$_2$=C$_3$=C$_4$H—]$_x$H

	x	$r_{C_1=C_2}$	$r_{C_2=C_3}$	$r_{C_3=C_4}$	r_{C-C}
butatriene	1	1.296	1.256	1.296	
dibutatriene	2	1.298	1.253	1.307	1.483
tributatriene	3	1.311	1.247	1.311	1.479

H[—HC$_1$=C$_2$=C$_3$=C$_4$=C$_5$=C$_6$H—]$_x$H

	x	$r_{C_1=C_2}$	$r_{C_2=C_3}$	$r_{C_3=C_4}$	$r_{C_4=C_5}$	$r_{C_5=C_6}$	r_{C-C}
hexapentaene	1	1.297	1.259	1.273	1.259	1.297	
dihexapentaene	2	1.299	1.257	1.277	1.253	1.312	1.477
trihexapentaene	3	1.315	1.249	1.283	1.249	1.315	1.474

[a] Their structure is schematized in Figure 13.

the repeat unit in a polymer. As already pointed out, the changes in the geometrical parameters of polyenes are qualitatively well predicted with the STO-3G basis as compared with more refined theoretical results. It might be useful to add that the main difference between STO-3G and 6-31G results lies in the fact that the STO-3G C=C and C—C bond lengths are systematically shorter and longer, respectively. Comparison of the theoretical data in Table IX with recent X-ray measurements on small cumulenes[60] substantiates the above comment: calculated bond lengths are 0.02 Å shorter than the experimental ones, but the trends are always respected. Thus, it is expected that the structural changes occurring in longer oligomers will be calculated at the same level of quality.

In the case of butatriene, dibutatriene, and tributatriene, the tendency for the longer chains to adopt a polyyne-like structure, (—C≡C—)$_n$, typical of the resonance form b is obvious and is in agreement with the calculations by Karpfen on the infinite chain.[41] This trend is also seen in the case of hexapentaene, dihexapentaene, and trihexapentaene. Not to be overlooked is the simultaneous reduction of the C–C bonds connecting the units. Thus the polarizability of these oligomers, which depends on the effectiveness of the delocalization over the entire backbone, is dependent on two effects: the changes in delocalization of the repeating units as the number of connected carbon atoms increases and the parallel trend for the C–C bonds connecting the repeating units to shorten. One can relate the geometry changes just discussed to the polarizability values listed in Table X.

When the number, k, of directly connected atoms in a cumulenic unit increases, the average polarizability, $\langle\alpha\rangle$, continues to increase, in spite of the slight tendency for the geometries to evolve toward form b of the two resonance structures. It is likely that saturation in monomeric units will occur in longer structures than the ones considered in this work. In the oligomers, the C–C distances connecting the repeat units tend to shorten with the net result of improving the delocalization of the π electrons. The overall effect is a continuous increase of the polarizability and the additivity regime is not yet reached in the case of the trimers. Thus, oligomers of cumulenic structures are highly polarizable systems, in fact more than the polydiacetylene and

TABLE X. STO-3G Average Polarizability, $\langle\alpha\rangle$ (in au), and Its Ratios with the Number of Electrons, n_e, π Electrons, n_π, Carbon Atoms, n_C, and Delocalization length, l_π (in Å)

	x	$\langle\alpha\rangle$	$\langle\alpha\rangle/n_e$	$\langle\alpha\rangle/n_\pi$	$\langle\alpha\rangle/n_C$	$\langle\alpha\rangle/l_\pi$
H[—HC$_1$=C$_2$H—]$_x$H						
ethylene	1	10.74	0.67	5.37	5.37	8.20
butadiene	2	25.15	0.84	6.29	6.29	6.85
hexatriene	3	43.93	1.00	7.32	7.32	7.17
H[—HC$_1$=C$_2$=C$_3$=C$_4$H—]$_x$H						
butatriene	1	30.19	1.08	5.03	7.55	7.84
dibutatriene	2	91.11	1.69	7.59	11.39	10.57
tributatriene	3	184.85	2.31	10.27	15.40	13.74
H[—HC$_1$=C$_2$=C$_3$=C$_4$=C$_5$=C$_6$H—]$_x$H						
hexapentaene	1	65.57	1.64	6.56	10.93	10.26
dihexapentaene	2	229.47	2.94	11.47	19.12	16.79
trihexapentaene	3	508.57	4.38	16.95	28.25	24.24

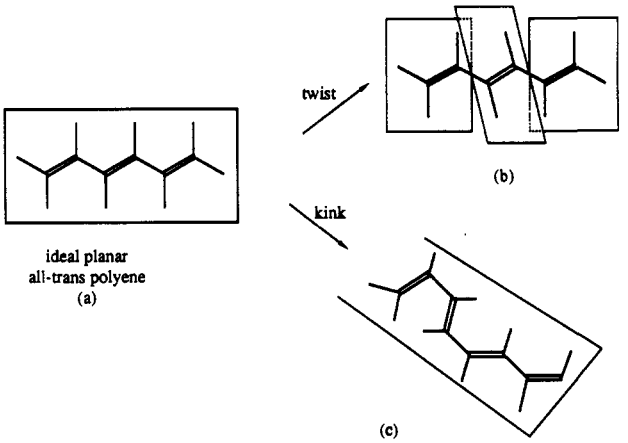

Figure 14. Schematic representation of possible structural defects that can occur in polyene chains.

polyene analogues. Again, when considering the cumulenic compounds one should not ignore problems related to their stability and optical properties (transparency).

C. Hydrogen-Bonded Systems

Controlling the structure at the molecular level, increasing the density of electroactive species, and improving the stability of the material are also very important aspects in the molecular engineering of new materials for optoelectronics. In this section, we illustrate contributions from quantum chemistry calculations to the question of controlling the molecular order. Experimentally, various approaches are currently considered to form materials with some organization at the molecular level; the most often used are Langmuir–Blodgett film deposition, topochemical solid-state polymerization, and liquid-crystal formation.

Molecular arrangements are dictated by the specific interactions existing between molecules; it should then be possible to select suitable chemical moieties, grafted to and/or incorporated in the conjugated backbone, to enforce intra- and interchain order and to some extent prevent structural defects from occurring. In long chains, conformational freedom can result in kinks and/or twists as shown in Figure 14 which disrupt the conjugation and thus spoil the expected benefit of the l_π^3 dependence (section V.B.1). The approach based on hydrogen bonding has received increased attention. For example, in the case of liquid–crystalline systems, chain ordering by hydrogen-bond formation has been pointed

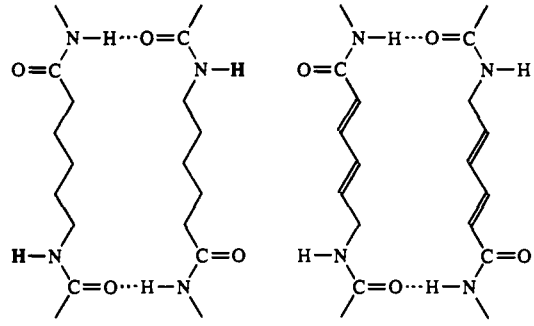

(a) (b)

Figure 15. Sketch of the hydrogen-bond pattern in (a) nylon 6 and (b) in its hypothetical conjugated analogue.

out. A more systematic use of hydrogen bonding as organizing forces in materials for optoelectronics has recently been considered theoretically[38,61] and experimentally.[62]

In this part we would like to consider, from a theoretical point of view, the possibility of using hydrogen bonds to prevent and/or minimize the occurrence of these undesirable structural defects and the more specific study of the intrinsic polarizability properties of some relevant hydrogen-bond patterns.[38] Before comparing the polarizability of several hydrogen-bond patterns, it can be of interest to indicate how the amide linkage could be used, both directly in the active backbone or as a terminal group, and explain the possible benefits of such changes.

Nylons owe part of their mechanical properties to hydrogen bonds which, among other things, induce a better organization at the molecular level. Figure 15 provides a schematic representation of the hydrogen-bonded sheets with amide groups in nylon 6 as inferred from crystal structure determination.[63] Provided organic chemists succeed in the preparation of the appropriate monomers, i.e., without encountering undue stability and reactivity problems, it could be conceivable to form by polycondensation the unsaturated analogues of nylon 6 as also shown in Figure 15. Again if the chemistry is tractable, longer chains could be incorporated between the amide groups with the expected benefit of locking the double bond sequence in a more ordered way and thereby minimize the occurence of kinks and twists in the conjugated backbone.

Another way of using hydrogen bonds is to increase the density of active species in a crystal by increasing the cohesive interactions and thereby force the conjugated backbones to order. For instance, it is known that muconic acid (**34**)[64] forms hydrogen bonds in the crystal; these bonds force the molecule to fully align owing to the cyclic hydrogen-bonded pairs between two carboxylic groups (see Figure 16a). On the contrary, *trans,trans*-dimethylmuconate (**35**)—which has a structure[65] close to that of muconic acid (**34**), but without the possibility of forming hydrogen bonds—exhibits a quite different organization in the crystal (see Figure 16b). There are many more examples of hydrogen-bond patterns that could be used to exert some control on the molecular organization of the active species.

Quantum chemistry can bring useful contributions to this question by calculations of the polarizability dependence on the structure of the isolated molecules,

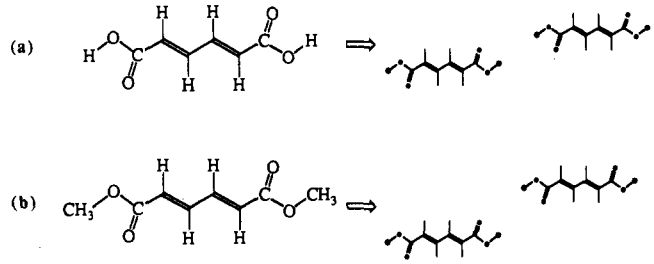

Figure 16. Sketch of the relative position of muconic acid (**34**) and *trans,trans*-dimethylmuconate (**35**) in their crystalline arrangement.

on the one hand, and the molecules interacting via hydrogen bonds, on the other hand. Properties of hydrogen-bonded molecules are difficult to obtain correctly with small basis set calculations. Additional problems concerning the comparison of isolated and interacting systems due to the so-called superposition error come into play. Thus, the results presented in this section should be considered with caution even though detailed calculations with larger basis sets show that from a qualitative point of view the STO-3G results are reasonable.[61a]

By ab initio calculations of the static electric dipole polarizability, we want to assess the relative efficiency of hydrogen-bond-forming molecules as transmitters of the electronic conjugation existing in a polyene chain. In this contribution we focus on oligomers of polyenes in which hydrogen-bond-forming chemical moieties are included to improve inter- and intrachain order as indicated in Figure 17. Full STO-3G geometry optimization has been carried out on the molecular systems (kept planar). Figure 18 shows the various molecular arrangements considered for each of the combinations of hydrogen-bonding molecules included in the reference conjugated hydrocarbon frameworks, C=CC=CX and C=CXC=C. Arrangement a corresponds to an isolated hydrogen-bond-forming molecule X (X = **36–40**, as indicated in Figure 17), **b** and **c** are isolated conjugated oligomers representative of a possible repeat unit of an actual polymer, where they differ by the position of the hydrogen-bond-forming molecule in the backbone. Most often, incorporating moieties structurally and/or chemically different from the repeating structure of the conjugated chain leads to a decrease in the effective delocalization (section V.A) which can be estimated from the polarizability changes. Thus, the purpose of considering arrangements **b** and **c** is to assess, by comparison, the extent of the interruption of the electronic conjugation due to the incorporation of a molecular fragment X at the end and in the middle of the butadienic backbone. Arrangements **d** and **e** should provide information on the influence of lateral interchain hydrogen bonds on the polarizability.

The total energy, E_T; the dipole moment, μ; the molecular volume, V; and the average polarizability divided by the molecular volume, αV^{-1} are listed in Table XI. Notation corresponds to that introduced in Figure 18. Stability difference between the isolated isomers, E_T(**b**) − E_T(**c**), or between the isomers laterally connected to two hydrogen-bonding molecules, E_T(**d**) − E_T(**e**), is negligible, about 1 kcal mol^{-1} or less. Similarly the volume changes in comparable arrangements **b**, **c** and **d**, **e** is not significant except for system **40**, where a 3% decrease from **40d** to **40e** is calculated.

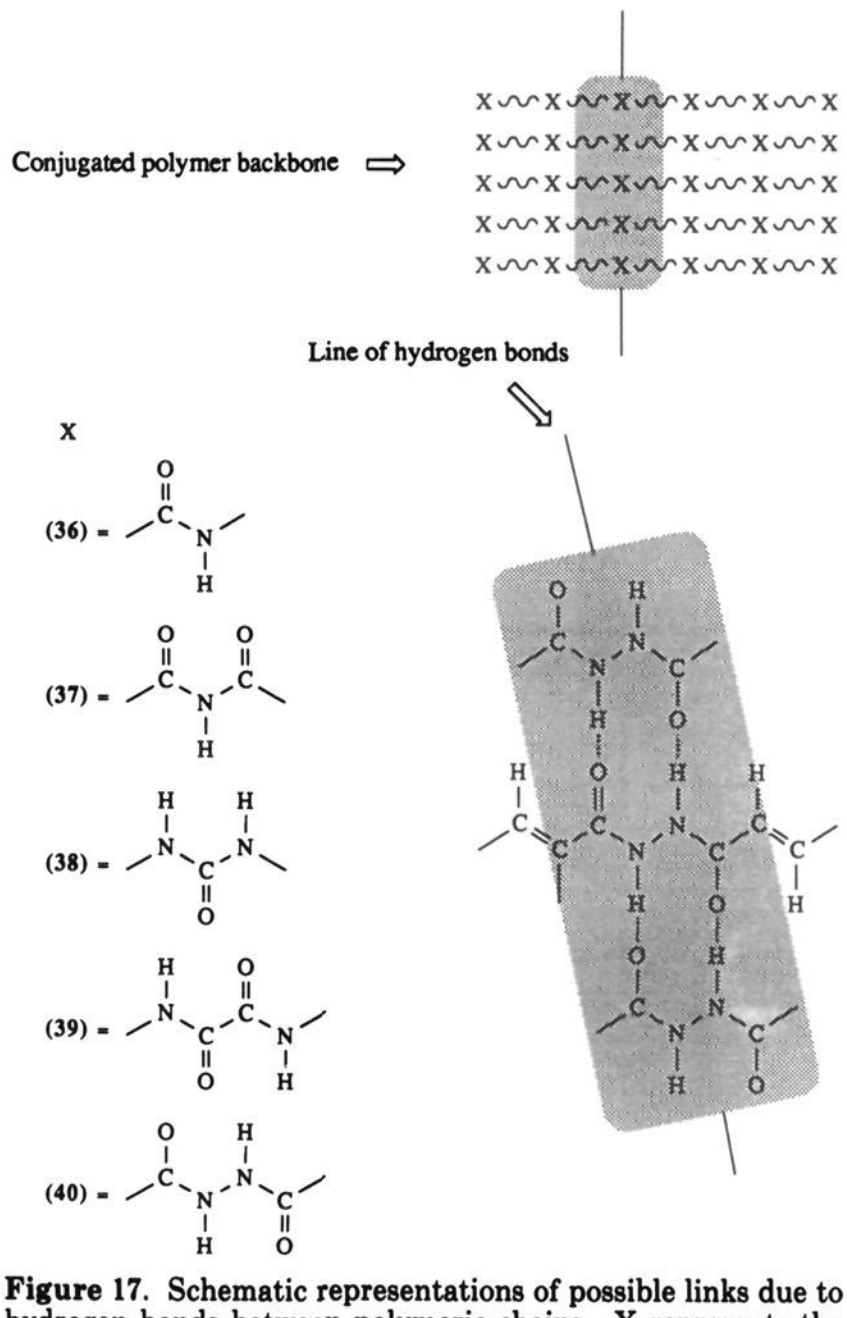

Figure 17. Schematic representations of possible links due to hydrogen bonds between polymeric chains. X represents the chemical moieties considered in this work. The shaded areas delineate the size of the molecular structures used to model locally the polymer situation.

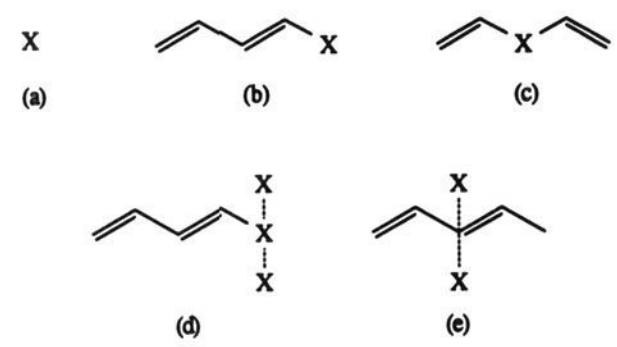

Figure 18. Schematic representation of (i) the five molecular arrangements (**a**–**e**) considered for each of the (ii) five systems of hydrogen-bonding molecules included in the reference conjugated hydrocarbon framework: C=CXC=C, C=CC=CX.

The dipole moment, when symmetry allows it, is moderately influenced by the position of the hydrogen-bond-forming moiety in the backbone, but it is more dependent on the existence of interchain hydrogen bonds. For instance, in system **36** the dipole moment ranges from 2.64 to 2.33 D for arrangements **a**–**c**, but it exceeds by more than 1.5 D the added contributions of three formamide molecules, $HCONH_2$, similarly oriented. For instance, in **e** μ (=9.53 D) is 1.6 D larger than the dipole moment of three formamide molecules. Similar trends are also observed in the case of systems **37**–**39**, the trend being less marked in the last two cases. The reverse situation is found for system **40**. Note that STO-3G dipole moments are almost always underestimated, but the trends are generally correct except in situations of very small dipoles or when the electronic structure cannot be correctly described within the single determinant approximation.

TABLE XI. Total Energy, E_T (in au), Dipole Moment, μ (in D), Molecular Volume, V (in Å^3), and Average Polarizability Divided by the Molecular Volume, αV^{-1} (in au Å^{-3}), for Systems 36–40

	E_T	μ	V	αV^{-1}
		System **36**		
36a	−166.68 821	2.64	41.88	0.25
36b	−318.58 177	2.44	96.60	0.40
36c	−318.58 183	2.34	94.69	0.38
36d	−651.97 386	9.95	179.63	0.35
36e	−651.97 374	9.53	178.29	0.34
		System **37**		
37a	−277.92 701	4.19	60.99	0.28
37b	−429.82 101	4.40	115.11	0.41
37c	−429.81 923	4.26	114.53	0.37
37d	−985.69 580	15.34	235.35	0.36
37e	−985.69 466	15.25	236.28	0.34
		System **38**		
38a	−221.01 671	3.16	51.77	0.27
38b	−372.91 111	3.18	107.25	0.42
38c	−372.91 099	2.62	105.21	0.40
38d	−814.97 200	12.94	212.11	0.37
38e	−814.97 174	12.63	211.51	0.35
		System **39**		
39a	−332.25 215	0.0	72.59	0.29
39b	−484.14 559	1.27	126.88	0.42
39c	−484.14 554	0.0	125.36	0.40
39d	−1148.67 355	1.31	266.27	0.39
39e	−1148.67 254	0.0	265.00	0.38
		System **40**		
40a	−332.20 027	0.0	74.15	0.30
40b	−484.094 71	1.25	126.75	0.42
40c	−484.09 360	0.0	127.89	0.38
40d	−1148.53 211	1.07	270.10	0.41
40e	−1148.53 086	0.0	262.23	0.40

The polarizability per unit volume, αV^{-1}, decreases only very slightly when the systems are laterally connected through hydrogen bonds; for instance, αV^{-1} is equal to 0.40 in **36a** and 0.35 in **36d**; similarly it is equal to 0.38 in **36c** and 0.34 in **36e**. There is also a systematic decrease in αV^{-1} when the hydrogen-bond-forming moiety is in the center of the reference conjugated hydrocarbon framework (C=CXC=C). For the isolated chains, the largest decrease is observed for systems **37** and **40**. When lateral hydrogen bonds are present as in arrangements **d** and **e**, αV^{-1} decreases in all systems except for system **40**, where αV^{-1} is somewhat larger, 0.40, in **40e** than in the isolated situation **40c**, 0.38.

The differences between the isolated molecules, [**b** + 2(**a**)] or [**c** + 2(**a**)], and those in interaction, **d** or **e**, are more easily understood from the results listed in Table XII. Two properties will be of interest to us here: the stabilization energy and the variation of polarizability. The stabilization energy is an important aspect to take into account, because a larger stabilization energy is generally more propitious for the desired aggregate structure to occur. Discussion of stabilization energy is always a difficult subject due to basis set superposition errors. On the basis of observations by various authors[66] and our own results on formic acid and formamide[61a] showing that the STO-3G stabilization energies are often comparable to results obtained with larger basis sets, we use in a straightforward manner the differences indicated in Table XII to compare the stabilization energies of the five systems

TABLE XII. Difference in Total Energy, ΔE_T (in kcal mol^{-1}), Dipole Moment, $\Delta\mu$ (in D), Molecular Volume, ΔV (in Å^3), and Average Polarizability, $\Delta\alpha$ (in au), between the Fully Interacting Systems (xd or xe) and the Sum of Contributions from the Isolated Parts [xb + 2(xa)] or [xc + 2(xa)] (x = 36–40)

	ΔE_T	$\Delta\mu$	ΔV	$\Delta\alpha$
	System 36			
36d – [36b + 2(36a)]	−9.81	2.22	−0.73	3.63
36e – [36c + 2(36a)]	−9.71	1.90	−0.16	3.74
	System 37			
37d – [37b + 2(37a)]	−13.03	2.55	−1.74	3.92
37e – [37c + 2(37a)]	−13.41	2.62	−0.23	3.61
	System 38			
38d – [38b + 2(38a)]	−17.38	3.41	+1.32	5.92
38e – [38c + 2(38a)]	−17.15	3.69	+2.76	5.80
	System 39			
39d – [39b + 2(39a)]	−15.98	0.04	−5.79	8.96
39e – [39c + 2(39a)]	−15.68	0.0	−5.54	8.35
	System 40			
40d – [40b + 2(40a)]	−23.14	−0.18	−4.95	11.48
40e – [40c + 2(40a)]	−23.05	0.0	−13.96	11.48

studied in this paper. In order of increasing stabilization energies, one finds **36 < 37 < 39 < 38 < 40**, while for polarizability gains, one has **36 ≈ 37 < 38 < 39 < 40**. It must be recalled at this point that in system **40** the disadvantage of incorporating a heteroatomic moiety in the C=CC=C backbone is partially removed due to the presence of neighboring hydrogen bonds.

When incorporated in the C=CC=C backbone, the hydrogen-bond-forming group —CONHNHCO— presents the most favorable stabilization energy and polarizability gain of the systems considered. It should be of interest in the design of new molecules for optoelectronics when forcing organization is seeked. In spite of the fact that the hydrazide group is not yet part of the extensive list of hydrogen-bond patterns recently published by Etter,[62b] several crystal determinations have been reported on hydrazide compounds. For instance, anhydrous diacetylhydrazine[67] is known to form molecular arrangements of the type shown in Figure 17. In the field of macromolecules, Rogers et al.[68] have reported a quite interesting and related work on linear unsaturated polyamides and polyhydrazides that should be valuable to develop in the framework of nonlinear optics.

D. Charge-Transfer Systems

Adding electron donating (accepting) atoms and/or molecules in a medium capable of accepting (donating) the electrons (n and/or p doping in the physicists' terminology) usually leads to charge-transfer complexes often characterized by geometry relaxations in the partner molecules. This process is extensively used to obtain conducting polymers. Provided charge transfer can be controlled, it may serve as an additional way to obtain molecules characterized by better delocalized π-electron networks and thus exhibiting enhanced electric responses.

Here we examine[69] three types of chains which have been extensively studied, namely, polyparaphenylene, polypyrrole, and polythiophene. Doping induces strong geometric modification of the aromatic polymer backbone toward a more quinoidlike structure. Since a quinoidic structure is expected to be more polarizable

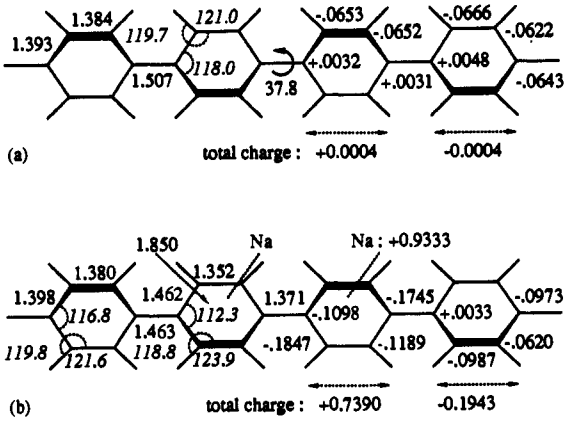

Figure 19. STO-3G-optimized geometry (bond lengths in Å and angles in degrees) and net Mulliken atomic charges on the carbon atoms (in units of the electronic charge) for (a) quaterphenyl for which D_2 symmetry is assumed and (b) sodium-doped quaterphenyl with C_2 symmetry assumed.

TABLE XIII. STO-3G Average Polarizability, $\langle\alpha\rangle$, and Its Cartesian Components, α_{xx}, α_{yy}, and α_{zz} (in au), for Quaterphenyl, Quaterpyrrole, and Quaterthiophene[a]

	α_{zz}	α_{yy}	α_{xx}	$\langle\alpha\rangle$
		Quaterphenyl		
A	291.17	145.59	39.26	159.34
B	790.00	153.50	26.14	323.21
C	482.45	160.00	22.35	221.60
D	210.13	0.02	0.03	70.06
E	692.58	160.02	22.38	291.66
		Quaterpyrrole		
A	224.65	135.09	15.94	125.23
B	534.15	137.62	20.03	230.60
C	352.42	135.34	15.97	167.91
D	141.07	13.25	0.02	51.45
E	493.49	148.49	15.99	219.36
		Quaterthiophene		
A	268.01	140.31	19.85	142.72
B	608.35	138.42	23.78	256.85
C	473.34	145.06	19.93	212.77
D	160.75	12.92	0.02	57.90
E	534.09	157.98	19.95	270.67

[a] A refers to the undoped tetramers, B corresponds to the tetramers doped with two Na atoms, C refers to the tetramers in the geometry of the doped oligomers, but in the absence of the corresponding Na dopants, D corresponds to the two Na atoms in the situation they have in the doped system, but without the tetramers, results in E are obtained by simply adding columnwise the results C and D. The z axis is perpendicular to the chain axis and the y axis is perpendicular to the average plane of the chain.

because, contrary to benzene, there is no aromaticity-driven stabilization to damp the electric response of the π electrons (see section V.B.2), it is interesting to study the influence of doping on the electric polarizability of representative oligomers quaterphenyl, quaterpyrrole, and quaterthiophene.

Geometry optimizations have been reported previously for these tetramers, undoped and doped with two Na atoms. The geometry changes when going from quaterphenyl to 2Na-doped quaterphenyl are shown in Figure 19; the other tetramers follow the same trends from the point of view of the geometry modifications resulting from doping.

It is easily observed that upon doping, the inner rings adopt a quinoidlike structure, the double bonds vary from 1.35 to 1.37 Å, and the single bonds vary from 1.43 to 1.46 Å.[70] The results for the average polarizability,

$\langle\alpha\rangle$, and its cartesian components, α_{xx}, α_{yy}, and α_{zz}, are given in Table XIII for quaterphenyl, quaterpyrrole, and quaterthiophene: (A) for the undoped oligomers, (B) for the oligomers doped with two sodium atoms, (C) for the systems in the geometry induced by the dopants, but the sodium atoms not included in the calculations, (D) for the two Na atoms only geometrically placed as in the doped situation, and (E) the sum of polarizability contributions from C and D, term by term.

In all cases A, B, C, and E quaterphenyl is found more polarizable than the other two tetramers. This is in line with the experimental polarizability of the three monomers which orders as benzene > thiophene > pyrrole.[71]

Doping induces a strong increase in polarizability. The average value $\langle\alpha\rangle$ doubles in the case of quaterphenyl and increases by about 80–85% in the heteroatomic systems. Note that the average polarizability is related by a 2.5-fold increase in the longitudinal polarizability, α_{zz}, the other components being almost unaffected by the doping process. From the results in situations C and D, the overall polarizability increase can be explained as originating from two factors: first, the geometry modifications toward a more polarizable quinoid-type structure (this accounts for two-thirds of the total polarizability increase); second, the increase of electronic charge on the carbon backbone due to electron transfer from the sodium atoms.

The significant increase of electric polarizability resulting from doping aromatic tetramers is expected to yield an even more important enhancement in the third-order polarizability if the assumptions on the scaling laws hold true.

One of the interesting problems in the linear and nonlinear optical properties of polymers is the influence of defects existing in the main chain. De Melo and Silbey have studied the effects of neutral and charged defects (solitons and polarons) on the polarizability and hyperpolarizabilities of polyenes.[72] According to their results, the polyenes with charged defects (charged solitons, charged polarons and bipolarons) exhibit remarkably greater polarizabilities α_{zz} (z is the chain direction) than those of regular polyenes. They find that the charged solitons and singly charged polarons are associated with a negative γ_{zzzz}, while in the regular polyene γ_{zzzz} is positive; the origin of these effects is not yet clear. Similar results are also reported by Nakane et al. using CNDO/S-CI and time dependent perturbation theory;[73] they also investigate the γ value of other polyenic systems.

Obviously, these prospects of using doping in the field of optoelectronics must also meet other requirements than just high electric responses. Other properties (transparency, radiation damage, etc.) must also be satisfied.

VI. The Problem of Infinite Chains

In the study of the perturbation due to the switching of an external electric field, it is anticipated that the polarizability, normalized to the monomeric unit, tends to reach an asymptotic limit which should grow when the systems exhibit increased geometrical regularity (metallic situation). For complex systems, this limit will soon be out of reach when studying chains of increasing length. An example is given in Figure 20, which graphically plots the trends of the longitudinal polarizability per unit cell (α_{zz}/n) as a function of the size of the system in tetrahedrally coordinated polymer chains: polyethylene and polysilane now recognized as a σ-conjugated chain. Thus, it is evident that calculations on oligomers of finite size cannot be used in order to get a reliable estimate of the polarizability per unit cell of the infinite chain (except in ideal cases), and it would be most useful to be able to estimate this limit from direct calculations on infinite chains.

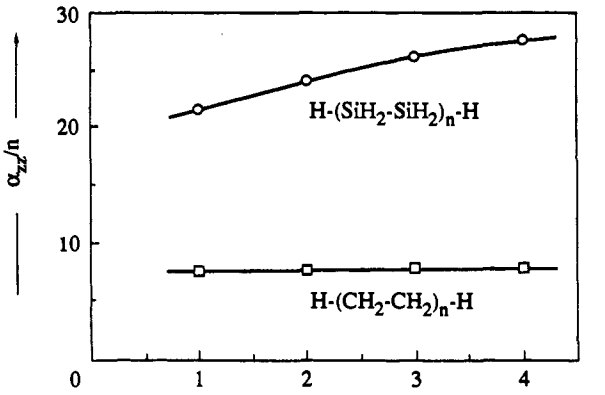

Figure 20. Polarizability per unit cell (α_{zz}/n) as a function of the size of the system in tetrahedrally coordinated polymer chains polyethylene and polysilane.

In a first step, it might seem rather trivial to replace simply field-dependent MO's by field-dependent Bloch polymeric orbitals and assume the usual periodicity properties. However, two types of questions are raised. On the one hand, as shown by Churchill and Holmstrom,[74] serious difficulties arise in imposing realistic boundary conditions to solve the one-electron eigenvalue equation; under the periodic boundary conditions commonly used in treating the zero-field case (i.e., Born–Karman boundary conditions), this equation either leads to physically inconsistent results or, still worse, has no solution at all. This strange behavior is a consequence of the pathological nature of the perturbing term, $-\mathbf{F}\cdot\mathbf{r}$, due to the external electric field $\mathbf{F}$ which becomes unbounded as $\mathbf{F} \to 0$ and $\mathbf{r} \to \infty$. As mentioned by Callaway,[75] it is evident that there will be difficulties associated with the application of perturbation theory because, for sufficiently large distances, the perturbation becomes arbitrarily large, no matter how weak the field is. Strictly speaking, there are no bound states when the hamiltonian contains a term of the form of $-\mathbf{F}\cdot\mathbf{r}$. On the other hand, the periodic character of the perturbation is not guaranteed under the nonperiodic linear external perturbation which would rule out the use of field-perturbed Bloch orbitals.

As far as we know, there is no coupled Hartree–Fock calculations on infinite polymers, so that in this section, we limit ourselves to the SOS (uncoupled Hartree–Fock) value of the frequency-independent longitudinal polarizability which, by its first approximation character, neglects the electron reorganizational effects due to the presence of an external electric field. Theoretical studies of the asymptotic limit of the polarizability of infinite model polymeric chains (chains of hydrogen atoms, polyacetylene, polydiacetylene, polyethylene, and polysilane) are described in the literature at the simple Hückel[76] and more elaborated ab initio[77] levels

TABLE XIV. STO-3G Polarizability Components of Alkane and Silane Chains, Longitudinal Polarizability per Unit Cell, and Their Asymptotic Limit (in au)

	total polarizability						polarizability per unit cell		
	polyethylene chains			polysilane chains					
no. of monomer units	α_{zz}	α_{xx}	α_{yy}	α_{zz}	α_{xx}	α_{yy}	no. of monomer units	polyethylene chains: α_{zz}/N	polysilane chains: α_{zz}/N
1	7.604	9.089	9.089	21.551	19.153	19.153	1	7.604	21.551
2	15.430	17.176	18.296	47.824	41.276	39.220	2	7.715	23.912
3	23.268	25.340	27.500	78.663	62.030	59.230	3	7.757	26.221
4	31.096	33.527	36.705	109.944	82.903	79.372	4	7.775	27.486
							polymer limit	7.770	28.630

using the SOS (summation-over-states) perturbative methodology of Genkin and Mednis.[78] The relation which defines the static dipole longitudinal polarizability per unit cell of a large oligomer extending along the z direction in terms of its MO's:

$$\frac{\alpha_{zz}}{N} = \frac{1}{N}\sum_i\sum_a \frac{|2\langle\phi_i|z|\phi_a\rangle|^2}{\epsilon_a - \epsilon_i} \tag{13}$$

(the summations are extended over all the occupied $\{i\}$ and unoccupied $\{a\}$ MO's) has to be transformed into the following formula for the calculation of the polymeric polarizability per unit cell:

$$\frac{\alpha_{zz}}{N} = \frac{2a}{\pi}\sum_i\sum_a \int_{BZ} dk \frac{|\Omega_{ia}(k)|^2}{\epsilon_a(k) - \epsilon_i(k)} \tag{14}$$

where

$$\frac{\Omega_{ia}(k)}{N} = \frac{1}{a}\int_{cell} d\mathbf{r} u_i^*(k,\mathbf{r})\frac{\partial}{\partial k}u_a(k,\mathbf{r}) \tag{15}$$

In the latter equation, $u_n(k,\mathbf{r})$ is the periodic part of the LCAO polymeric Bloch function:

$$\phi_n(k,\mathbf{r}) = \frac{1}{\sqrt{N}}\sum_j e^{ikja}\sum_p c_{np}(k)\chi_p(\mathbf{r} - \mathbf{P} - ja) \tag{16a}$$

$$= e^{ikz}\frac{1}{\sqrt{N}}\sum_j e^{ik(ja-z)}\sum_p c_{np}(k)\chi_p(\mathbf{r} - \mathbf{P} - ja) \tag{16b}$$

$$= e^{ikz}u_n(k,\mathbf{r}) \tag{16c}$$

where N is the (odd) number of unit cells in the polymer, n the band index, $\mathbf{r}$ the position vector, k the wave number in the first Brillouin zone ($-\pi/a \le k \le \pi/a$), $\mathbf{P}$ the position of the center of orbital χ_p in the unit cell of length a, and j the cell index. The standard theory of band-structure calculations is described in several papers[79] and is reviewed in two recent monographs.[80] The transformation of the matrix elements of the coordinate z of the molecular case $\langle\phi_i|z|\phi_a\rangle$ or of the polymeric Bloch case $\langle\phi_n(k)|z|\phi_{n'}(k')\rangle$ into the vertical matrix elements of the k gradient $\partial/\partial k$ involving the periodic parts of the Bloch functions $u_n(k,\mathbf{r})$ is given in several books.[75,81]

We exemplify this section by the examples of polyethylene and polysilane chains. In Table XIV, we present the SOS polarizabilities of some alkane and silane oligomers. The x and y axes are perpendicular to the polymer backbone while the z axis is along the periodicity direction.

We note the higher polarizabilities of the silicon compounds, already pointed out by many authors and associated with the greater volume of the silicon atom and the σ conjugation present in the silanes. More interesting are the longitudinal polarizabilities per unit cell given in the second part of Table XIV. The van der Waals volumes for the monomer units are 268.5 and 403.1 au^3, respectively. The ratio (α/V multiplied by 100) is larger for polysilane (7.10) than for polyethylene (2.89). It is important to note that in the alkane chains, the effect of the chain size turns out to be almost strictly additive as already illustrated in Figure 20. In the silane chains, on the other hand, there is a saturation pattern and the asymptotic limit is not reached after the first few terms, a clear indication of a σ-conjugation effect. From a methodological point of view, it again indicates the need for developing accurate techniques of calculation for the asymptotic limit of the longitudinal polarizability. The asymptotic limit (polymeric limit) of the longitudinal polarizability per unit cell is obtained from the ab initio STO-3G band structure by using the SOS–Genkin–Mednis approach.

A complete analysis of the band structures of polyethylene and polysilane in terms of minimal valence basis sets (1s for hydrogen, 2s, 2px, 2py, and 2pz for carbon, plus 3s, 3px, 3py, and 3pz for silicon) and in terms of bond orbitals has been recently given.[55b] In this study, in order to simplify the analysis, use has been made of the helical symmetry of the polyethylene chain. Polyethylene (or polysilane) can be considered as a zigzag linear polymer with a $-(CH_2CH_2)_n-$ (or with a $-(SiH_2SiH_2)_n-$) unit cell or as a 1*2/1 helix with an elementary asymmetric unit cell $-(CH_2)_n-$ (or $-(SiH_2)_n-$). The interpretive effort is also greatly simplified if one considers a priori the asymmetric unit as the relevant unit for the calculation. The successive displacements of the asymmetric unit involve, at the same time, the translation *and* the rotation of the atomic orbitals basis sets. The linear zigzag case is treated with a unit cell twice the size of the helical case, so that in the reciprocal space, the linear polyethylene or polysilane have a reciprocal unit cell and hence a first Brillouin zone half the size of the helical case. The band structure of the elementary asymmetric unit cell $-(CH_2)_n-$ (or $-(SiH_2)_n-$) is obtained by unfolding, in the linear case, the energy bands according to the symmetry requirements. The "folding back" of the dispersion curves for the six valence electrons (three electron pairs) contained in the asymmetric cell $-(CH_2)_n-$ (or $-(SiH_2)_n-$) gives the dispersion curves for the 12 valence electrons (six electron pairs) of the symmetric unit $-(CH_2CH_2)_n-$ (or $-(SiH_2SiH_2)_n-$) represented in Figure 21 which also defines the numbering of the bands and plots the structure of the first conduction bands.

In the sense of the previous discussion, bands 3 and 4, 5 and 6, 7 and 8 of the symmetric unit of polyethylene corresponds to the "folding back" of the three valence bands of the asymmetric cell $-(CH_2)_n-$. The same is

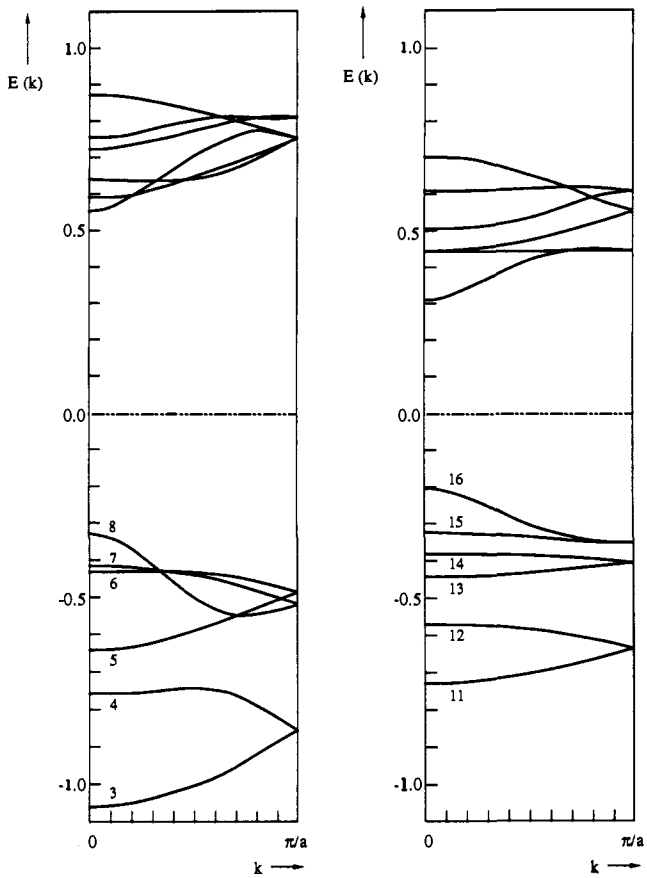

Figure 21. ab Initio STO-3G band structure of polyethylene (left) and polysilane (right).

true for bands 11 and 12, 13 and 14, and 15 and 16 of polysilane. In a simple picture consisting of chemical bonds, the orbital basis set of the asymmetric unit cell of polyethylene (or polysilane) contains two C–H (or Si–H) bonding orbitals and one C–C (or Si–Si) bonding orbital.

The following are clear from symmetry considerations.

1. The symmetric combination (with respect to the –CC– or –SiSi– backbone) of the C–H (or of the Si–H) orbital will combine with the C–C (or Si–Si) bond orbital. In the standard LCAO scheme, only the symmetric orbitals of the backbone atoms, i.e., C_{2s}, C_{2px}, and C_{2pz} (or Si_{3s}, Si_{3px}, and Si_{3pz}) interact with the symmetric combination of H_{1s}; they produce bands 3 and 4 and 7 and 8 of polyethylene (bands 11 and 12 and 15 and 16 in the case of polysilane).

2. The antisymmetric combination (with respect to the same –CC– or –SiSi– chain backbone) of the same C–H (or of the Si–H) orbital will not combine with the C–C (or Si–Si) bond orbital. This implies that in this simple model, the antisymmetric band has no contribution from the backbone. In the standard LCAO scheme, only C_{2py} (or Si_{3py}) interacts with the antisymmetric combination of H_{1s}. They correspond to bands 5 and 6 of polyethylene and bands 7 and 8 of polysilane. In particular, bands 7 and 8 of polyethylene (15 and 16 of polysilane) are antibonding combinations of the C–H (or the Si–H) orbital and of the C–C (or Si–Si) bond orbital. Band 7 of polyethylene (band 15 of polysilane) is dominated at $k = 0$ by the C–H (or Si–H) orbitals. Recalling that band 7 (from $k = 0 \rightarrow \pi/a$) and band 8 (from $k = \pi/a \rightarrow k = 0$) of polyethylene (bands 15 and 16 of polysilane) are the two branches of the same valence band within the asymmetric cell $-(CH_2)_n-$ (or $-(SiH_2)_n$), their analysis shows that they gradually transform into an antisymmetric (with respect to the plane of the zigzag chain) combination of the C–C (or Si–Si) bond orbitals. The previously mentioned paper[55b] demonstrates the important fact now experimentally proved[82] that at $k = 0$, the HOMO (band 8 of polyethylene or band 16 of polysilane) has no contribution from the C–H (or the Si–H) orbitals. The latter statement is important since it is generally believed that the HOMO of the tetrahedrally σ-bonded chains has mainly an X–H character. It is now clear that it is mainly an X–X bond orbital with nodes on each atom of the chain. This result is fully confirmed by inspection of the LCAO coefficients obtained in the minimal basis set calculation; the HOMO orbitals have only C_{2pz} contributions in polyethylene or Si_{3pz} contributions in the case of polysilane (remember that z is the chain axis).

TABLE XV. STO-3G Contributions of the Valence-Occupied Bands to the Longitudinal Asymptotic Polarizability per Unit Cell for Polyethylene and Polysilane Chains (in au)

polyethylene		polysilane	
band	contribution	band	contribution
3 (A_1)	0.011	11 (A_1)	0.159
4 (B_1)	0.012	12 (B_1)	0.094
5 (B_2)	0.065	13 (B_2)	0.190
6 (A_2)	0.288	14 (A_2)	0.190
7 (A_1)	2.938	15 (A_1)	6.562
8 (B_1)	4.363	16 (B_1)	21.410

As seen from eq 14, the polarizability per unit cell can be separated into contributions from each occupied band i, due to the structure of the summations of the Genkin–Mednis formula. An interesting feature is, thus, to relate the topology of each band and their contribution to the electric polarizability.[75e] In Table XV, we report the contributions of each occupied Bloch valence orbital of polyethylene and polysilane according to the labeling detailed in Figure 21. The core bands (bands 1 and 2 of polyethylene, and bands 1–10 of polysilane) contribute very weakly. Particularly interesting are the values of the two upper bands (bands 7 and 8). In both polymers, these two bands contribute most to the longitudinal polarizability (94.0% in the case of polyethylene and 97.7% in the case of polysilane). As just mentioned, the HOMO level corresponds to C_{2p} and Si_{3p} oriented along the chain axis. This peculiar topology, added to the large orbital polarizability of the 3p orbitals of silicon, is probably responsible for the σ conjugation of polysilanes. Finally, a rough estimate of the electron effective mass (another measure of the curvature near the HOMO) can also be made from the analytical curve near the HOMO level; we find that the electron effective mass is negative according to the bonding (stabilizing) character of the interactions involved; not forgetting the unit cell size effect, the numerical values of the variables which defines the denominator of the effective mass, m^* are in the ratio polyethylene/polysilane = 1.50;[55b] the effective mass of polyethylene is thus 1.5 times more important than that of polysilane, a result in complete agreement with the calculated values of Teramae and Takeda.[83] In their paper, the actual values of the effective masses were obtained in a different numerical way but the

effective masses of polysilane (0.14) and of polyethylene (0.21) are found to be in the same ratio 1.50 = 0.21/0.14. This leads to a large slope of the B_1 band near $k = 0$ for polysilane in agreement with the ratio of the effective masses (m^*) polysilane/polyethylene = 1.50.

In addition to polysilane, other conjugated inorganic polymers are also interesting for nonlinear optical materials. For example, polyphosphazenes which have a large degree of bond polarity in the main chain[84] can be expected to show large nonlinear optical responses. Risser and Ferris investigated a series of phosphonitrilic compounds for their third-order hyperpolarizabilities using the Hückel hamiltonian.[85] They reported that the electron-drawing nature of substituent groups remarkably affects the magnitude of γ and the onset of their saturation with increasing chain length for those molecules.

VII. Concluding Remarks

Definite successful theoretical and experimental achievements have been made in the area of the first hyperpolarizability (β). Reliable semiquantitative results can be obtained from theory for β, and calculations are routinely performed with a quite acceptable level of confidence to help designing new compounds for optoelectronics. The same cannot be claimed for the second nonlinear hyperpolarizability (γ), where both theory and experiment are at a very early stage of the understanding of the underlying processes in second-order effects.

Third-order electric responses are quite difficult to compute ab initio, even for very small systems. With very few exceptions, ab initio calculations in this field are presently limited to estimates of the static polarizability. However, the electronic and optical behavior of active main-chain polymers are basically related to the excited electronic states and their nature. For instance, Tokura et al. observed the electroreflectance (ER) spectrum of DFMDP (Polydiacetylene substituted with 2,5-bis(trifluoromethyl)benzene) and assigned a peak to the ^1A_g exciton which is on the higher energy side of the lowest ^1B_u exciton.[86] Further, they determined the oscillator strength between the ^1B_u and ^1A_g states by the measurement of the Stark shift of the ^1B_u state. Using these experimental parameters, they calculated the dispersion curve for the third-order nonlinear susceptibility for the first time. Their result predicts a strong resonance dispersion due to the two-photon transition to the ^1A_g exciton and an exceptionally large nonlinear refractive index in the near-infrared wavelength region. To deal with such problems, theoretical advances toward clever methodologies and efficient computer programs for reliable estimates of dynamical electrical responses of interesting systems for optoelectronics are needed and constitute a real challenge for present day quantum chemistry.

In the case of infinite polymers, we have shown that first-order techniques of computing the asymptotic longitudinal polarizabilities per unit cell of polymers exist. However, it is important to recognize the limitations of such methods which still do not take into account the field-induced coupled-reorganizational effects and the electron correlation. Coupled Hartree–Fock like methods would explicitly consider this electronic reorganization while the correlation effects could be included by example by the use of the polarization propagator techniques. Work in these directions is urgently needed.

Acknowledgments. This paper owes much to the colleagues we have collaborated with for many years and who impacted so much on us in the field of quantum chemistry applied to optoelectronics: Gaston Berthier, Jean-Luc Brédas, Michel Dupuis, John Morley, and Joseph Zyss. We had the pleasure of working with the following collaborators who gave advice and deeply contributed to the materials presented here: Christian Barbier, Vincent Bodart, Benoit Champagne, Magdalena Dory, Joseph Fripiat, Daniel Vercauteren, and Elie Younang. All the calculations reported here have been made on the Namur-Scientific Computing Facility (Namur-SCF), a result of the fruitful cooperation between the Belgian National Fund for Scientific Research (FNRS), IBM-Belgium, and the Facultés Universitaires Notre-Dame de la Paix (FUNDP). The work presented in this paper would not have been possible without the support of the ESPRIT-EEC under the successive contracts No. 443 "Molecular Engineering for Optoelectronics" (ESPRIT-Phase 1) and No. 2284 on "Optoelectronics with Active Organic Molecules" (ESPRIT-Phase 2).

References

(1) Blau, W. *Phys. Technol.* **1987**, *18*, 250.
(2) (a) Williams, D. J. (Ed.) *Nonlinear Optical Properties of Organic and Polymeric Materials*; ACS Symposium Series 233; American Chemical Society: Washington, DC, 1983. (b) William, D. J. *Angew. Chem. Int. Ed. Engl.* **1984**, 690. (c) Zyss, J. *J. Mol. Electron.* **1985**, *1*, 25. (d) Singer, K. D.; Lalama, S. D.; Sohn, J. E. *SPIE Integr. Opt. Circuit Eng. II* **1985**, *578*, 130. (e) Chemla, D. S. *Nonlinear Optical Properties of Organic Molecules and Crystals*; Zyss, J., Eds.; Academic Press: New York, 1987; Vol. 1 and 2. (f) Messier, J.; Kazjar, F.; Prasad, P.; Ulrich, D. (Eds.) *Nonlinear Optical Effects in Organic Polymers*; Kluwer Academic Publishers: Dordrecht, 1989.
(3) (a) Bloembergen, N. *Nonlinear Optics*; J. Wiley & Sons: New York, 1965. (b) Shen, Y. R. *The Principles of Nonlinear Optics*; J. Wiley & Sons: New York, 1984. (c) Reintjes, J. *Nonlinear Optical Parametric Processes in Liquids and Gases*; Academic Press: New York, 1984. (d) Munn, R. W. *J. Mol. Electron.* **1988**, *4*, 31.
(4) Zyss, J. In *Conjugated Polymeric Materials: Opportunities in Electronics, Optoelectronics, and Molecular Electronics*; Brédas, J. L., Chance, R. R., Eds.; Kluwer Academic Press: Dordrecht, 1990; p 545.
(5) (a) Roberts, G. G. *Adv. Phys.* **1985**, *34*, 475. (b) Peterson, I. R.; Girling, I. R. *Sci. Prog. (Oxford)* **1985**, *69*, 533. (c) Peterson, I. R. *J. Phys. D: Appl. Phys.* **1990**, *23*, 379.
(6) Möhlmann, G. R. *Europhys. News* **1990**, *21*, 83.
(7) Kowel, S. T.; Liangxiu Ye; Yixiang Zhang; Hayden, L. M. *Opt. Eng.* **1987**, *26*, 107.
(8) Spangler, C. W.; Hall, T. J.; Liu, P. K.; Dalton, L. R.; Polis, D. W.; Yu, L. In *Organic Materials for Non-Linear Optics*; Bloor, D., Hann, R. A., Eds.; Royal Society of Chemistry: London, 1991.
(9) Hameka, H. F. *J. Chem. Phys.* **1977**, *67*, 2935.
(10) Flytzanis, C. *ACS Symp. Ser.* **1983**, *233*, 167.
(11) Li, D.; Ratner, M. A.; Marks, T. J. *J. Am. Chem. Soc.* **1988**, *110*, 1707.
(12) Beratan, D. N. *J. Phys. Chem.* **1989**, *93*, 3915.
(13) Dirk, C. W.; Twieg, R. J.; Wagnière, G. *J. Am. Chem. Soc.* **1986**, *108*, 5387.
(14) (a) Zyss, J. *J. Chem. Phys.* **1979**, *70*, 3333. (b) Zyss, J. *J. Chem. Phys.* **1979**, *70*, 3341. (c) Zyss, J. *J. Chem. Phys.* **1980**, *71*, 909. (d) Zyss, J.; Berthier, G. *J. Chem. Phys.* **1982**, *77*, 3635.
(15) Wu, J. W.; Heflin, J. R.; Norwood, R. A.; Wong, K. Y.; Zamani-Khamiri, O.; Garito, A. F.; Kalyanaraman, P.; Sounik, J. *J. Opt. Soc. Am. B* **1989**, *6*, 707.
(16) Morley, J. O.; Docherty, V. J.; Pugh, D. *J. Mol. Electron.* **1989**, *5*, 117.
(17) Waite, J.; Papadopoulos, M. G. *J. Phys. Chem.* **1989**, *93*, 43.
(18) Pierce, B. M. *J. Chem. Phys.* **1989**, *91*, 791.
(19) Svendsen, E. N. *Int. J. Quantum Chem. Symp.* **1988**, *22*, 477.

(20) Parkinson, W. A.; Zerner, M. C. *Chem. Phys. Lett.* **1987**, *139*, 563.
(21) Williams, G. R. J. *J. Mol. Electron.* **1990**, *6*, 99.
(22) Bishop, D. M.; Pipin, J.; Rérat, M. *J. Chem. Phys.* **1990**, *92*, 1902.
(23) Shelton, D. P. *J. Opt. Soc. Am. B* **1989**, *6*, 830.
(24) Maroulis, G.; Thakkar, A. J. *J. Chem. Phys.* **1988**, *88*, 7623.
(25) Oddershede, J. *Advances in Chemical Physics*; Prigogine, I., Rice, S. A., Eds.; J. Wiley & Sons: New York, 1987; Vol. LXIX, Part II, p 201.
(26) Jensen, H. J. Aa.; Koch, H.; Jørgensen, P.; Olsen, *J. Chem. Phys.* **1988**, *19*, 297.
(27) Kirtman, B. *Int. J. Quantum Chem.* **1989**, *36*, 119.
(28) Karna, S. P.; Dupuis, M.; Perrin, E.; Prasad, P. N. *J. Chem. Phys.* **1990**, *92*, 7418.
(29) Cohen, H. D.; Roothaan, C. C. J. *J. Chem. Phys.* **1965**, *43*, S34.
(30) (a) Hartree, D. R. *Proc. Cambridge Philos. Soc.* **1928**, *24*, 89. (b) Hartree, D. R. *Proc. Cambridge Philos. Soc.* **1928**, *24*, 116. (c) Hartree, D. R. *Proc. Cambridge Philos. Soc.* **1928**, *24*, 426. (d) Hartree, D. R. *Proc. Cambridge Philos. Soc.* **1929**, *25*, 225. (e) Hartree, D. R. *Proc. Cambridge Philos. Soc.* **1929**, *25*, 310.
(31) Fock, V. *Z. Phys.* **1930**, *61*, 126.
(32) (a) Slater, J. C. *Phys. Rev.* **1929**, *34*, 1293. (b) Slater, J. C. *Phys. Rev.* **1930**, *35*, 509.
(33) Frisch, M. J.; Binkley, J. S.; Schlegel, H. B.; Raghavachari, K.; Martin, R. L.; Stewart, J. J. P.; Bobrowicz, F. W.; DeFrees, D. J.; Seeger, R.; Whiteside, R. A.; Fox, D. J.; Fleuder, E. M.; Pople, J. A. *Gaussian 86*, release C, Carnegie-Mellon University: Pittsburgh PA, 1984.
(34) (a) Hurst, G. J. B.; Dupuis, M.; Clementi, E. *J. Chem. Phys.* **1988**, *89*, 385. (b) Chopra, P.; Carlacci, L.; King, H. F.; Prasad, P. N. *J. Phys. Chem.* **1989**, *93*, 7120.
(35) (a) Davidson, E. R.; Feller, D. *Chem. Rev.* **1986**, *86*, 681. (b) Spackman, M. A. *J. Phys. Chem.* **1989**, *93*, 7594.
(36) Hehre, W. J.; Radom, L.; Schleyer, P. v. R.; Pople, J. A. *Ab initio Molecular Orbital Theory*; J. Wiley & Sons: New York, 1986.
(37) (a) Chablo, A.; Hinchliffe, A. *Chem. Phys. Lett.* **1980**, *72*, 149. (b) Bodart, V. P.; Delhalle, J.; Andrê, J. M.; Zyss, J. *Can. J. Chem.* **1985**, *63*, 1631. (c) Younang, E.; Delhalle, J.; Andrê, J. M. *New. J. Chem.* **1987**, *11*, 403.
(38) Delhalle, J.; Dory, M.; Fripiat, J. G.; Andrê, J. M. In *Nonlinear Optical Effects in Organic Polymers*; Messier, J.; Kazjar, F.; Prasad, P.; Ulrich, D., Eds.; Kluwer Academic Publishers: Dordrecht, 1989; p 13.
(39) Bodart, V. P.; Delhalle, J.; Andrê, J. M.; Zyss, J. In *Polydiacetylenes: Synthesis, Structure and Electronic Properties*; Bloor, D., Chance, R. R., Eds.; Martinus Nijhoff: Dordrecht, 1985; p 125.
(40) (a) Tokura, Y.; Oowaki, Y.; Koda, T.; Baughmann, R. H. *Chem. Phys. Lett.* **1984**, *88*, 437. (b) Kobelt, D.; Paulis, E. F. *Acta Crystallogr.* **1973**, *B30*, 232. (c) Enkelmann, V.; Lando, J. B. *Acta Crystallogr.* **1978**, *B34*, 2352.
(41) Karpfen, A. *J. Phys. C* **1980**, *13*, 5673.
(42) Flytzanis, C. In *Nonlinear Optical Properties of Organic Molecules and Crystals*; Chemla, D. S., Zyss, J., Eds.; Academic Press: New York, 1987.
(43) Bodart, V. P.; Delhalle, J.; Andrê, J. M. In *Conjugated Polymeric Materials: Opportunities in Electronics, Optoelectronics, and Molecular Electronics*; Brêdas, J. L., Chance, R. R., Eds.; Kluwer Academic Press: Dordrecht, 1990; p 509.
(44) (a) Smith, D. L.; Luss, H. R. *Acta Crystallogr.* **1972**, *B28*, 2793. (b) Smith, D. L.; Luss, H. R. *Acta Crystallogr.* **1975**, *B31*, 402.
(45) Bigelow, R. W.; Freund, H. J. *Chem. Phys.* **1986**, *107*, 159.
(46) (a) Kuhn, H. *Chim. Aarau* **1948**, *2*, 1. (b) Kuhn, H. *J. Chem. Phys.* **1948**, *16*, 840. (c) Kuhn, H. *Helv. Chim. Acta* **1948**, *31*, 1441. (d) Kuhn, H. *J. Chem. Phys.* **1949**, *17*, 1198. (e) Kuhn, H. *Chim. Aarau* **1955**, *9*, 237. (f) Kuhn, H. *Angew. Chem.* **1959**, *71*, 93.
(47) Andrê, J. M. Etude Comparative des Méthodes de Hückel et de l'Electron Libre. B.Sc. Thesis, U.C.L. Louvain, 1965.
(48) (a) Mee, J. D. *J. Am. Chem. Soc.* **1974**, *96*, 4712. (b) Mee, J. D. *J. Org. Chem.* **1977**, *42*, 1035. (c) Mee, J. D.; Sturmer, D. M. *J. Org. Chem.* **1977**, *42*, 1041.
(49) (a) Delhalle, J.; Bodart, V. P.; Dory, M.; Andrê, J. M.; Zyss, J. *Int. J. Quantum Chem.* **1986**, *19*, 313. (b) Bodart, V. P.; Delhalle, J.; Dory, M.; Fripiat, J. G.; Andrê, J. M. *J. Opt. Soc. Am.* **1987**, *B4*, 1047. (c) Baratan, D. N.; Onuchic, J. N.; Perry, J. W. *J. Phys. Chem.* **1987**, *91*, 2696. (d) Kirtman, B.; Hasan, M. *Chem. Phys. Lett.* **1989**, *157*, 123.
(50) Delhalle, J.; Champagne, B.; Dory, M.; Fripiat, J. G.; Andrê, J. M. *Bull. Soc. Chim. Belges* **1989**, *98*, 811.
(51) (a) Harrah, L. A.; Zeigler, J. *Macromolecules* **1987**, *20*, 601. (b) Kepler, R. G. *Synth. Met.* **1989**, *28*, C573. (c) Zeigler, J. M.; Gordon Fearon, F. W., Eds. *Silicon Based Polymer Science, A Comprehensive Resource*; Advances in Chemistry Series, 224; American Chemical Society: Washington, DC, 1990.
(52) (a) Kajzar, F.; Messier, J.; Rosilio, C. *J. Appl. Phys.* **1986**, *24*, 3040. (b) Yang, L.; Wang, Q. Z.; Ho, P. P.; Dorsinville, R.; Alfano, R. R.; Zou, W. K.; Yang, N. L. *Appl. Phys. Lett.* **1988**, *53*, 1245. (c) Schellenberg, F. M.; Byer, R. L.; Miller, R. D. *Chem. Phys. Lett.* **1990**, *166*, 331.
(53) Bigelow, R. W.; McGrane, K. M. *J. Polym. Phys.* **1986**, *24*, 1233.
(54) (a) Binkley, J. S.; Pople, J. A.; Hehre, W. J. *J. Am. Chem. Soc.* **1980**, *102*, 939. (b) Chandrasekhar, J.; Andrade, J. G.; Schleyer, P. v. R. *J. Am. Chem. Soc.* **1981**, *103*, 5609. (c) Gordon, M. S.; Binkley, J. S.; Pople, J. A.; Pietro, W. J.; Hehre, W. J. *J. Am. Chem. Soc.* **1982**, *104*, 2797.
(55) (a) Teramae, H.; Takeda, K. *J. Am. Chem. Soc.* **1989**, *109*, 1281. (b) Andrê, J. M. *Int. J. Quantum Chem., Quantum Chem. Symp.* **1990**, *24*, 65.
(56) Dory, M.; Beudels, L.; Delhalle, J.; Andrê, J. M.; Dupuis, M. *Int. J. Quantum Chem.* (issue in honour of E. Clementi), accepted.
(57) Bock, C. W.; Trachtman, M. J. *J. Mol. Struct. (THEOCHEM)* **1984**, *1*, 109.
(58) Teramae, H. *J. Am. Chem. Soc.* **1987**, *109*, 4140.
(59) Dewar, M. J. S. *J. Am. Chem. Soc.* **1984**, *106*, 669.
(60) Irngartinger, H.; Götzmann, W. *Angew. Chem. Int. Ed. Engl.* **1986**, *25*, 340.
(61) (a) Dory, M.; Delhalle, J.; Fripiat, J. G.; Andrê, J. M. *Int. J. Quantum Chem. Symp.* **1987**, *14*, 85. (b) Waite, J.; Papadopoulos, M. G. *Chem. Phys. Lett.* **1985**, *114*, 539. (c) Waite, J.; Papadopoulos, M. G. *Z. Naturforsch.* **1987**, *43a*, 253. (d) Waite, J.; Papadopoulos, M. G. *Can. J. Chem.* **1988**, *66*, 1440. (e) Papadopoulos, M. G.; Waite, J. *J. Chem. Soc., Faraday Trans. 2* **1989**, *85*, 1885. (f) Yasukawa, T.; Kimura, T.; Uda, M. *Chem. Phys. Lett.* **1990**, *169*, 259.
(62) (a) Panunto, T. W.; Urbanczyk-Lipkowska, L.; Johnson, R.; Etter, M. C. *J. Am. Chem. Soc.* **1987**, *109*, 7786. (b) Etter, M. C. *Acc. Chem. Res.* **1989**, *23*, 120. (c) Staab, E.; Addadi, L.; Leiserowitz, L.; Lahav, M. *Adv. Mat.* **1990**, *2*, 40.
(63) Parker, J. P.; Lindenmeyer, P. H. *J. Appl. Polym. Sci.* **1977**, *21*, 821.
(64) Bernstein, J.; Leiserowitz, L. *Isr. J. Chem.* **1972**, *10*, 601.
(65) Filippakis, S. E.; Leiserowitz, L. *J. Chem. Soc. B* **1967**, 290.
(66) (a) Sapse, A. M.; Fugler, L. M.; Cowburn, D. *Int. J. Quantum Chem.* **1986**, *29*, 1241. (b) Sauer, J.; Hobza, P.; Zahradnik, R. *J. Phys. Chem.* **1980**, *84*, 3318.
(67) Shintani, R. *Acta Crystallogr.* **1960**, *13*, 609.
(68) Rogers, H. G.; Gaudania, R. A.; Manello, J. S.; Sahatjian, R. A. *J. Macromol. Sci.—Chem.* **1986**, *A23*, 711.
(69) Dory, M.; Bodart, V. P.; Delhalle, J.; Andrê, J. M.; Brêdas, J. L. *Mat. Res. Soc. Symp. Proc.* **1988**, *109*, 239.
(70) Brêdas, J. L.; Thêmans, B.; Fripiat, J. G.; Andrê, J. M.; Chance, R. R. *Phys. Rev.* **1984**, *B29*, 6761.
(71) Le Fèvre, C. G.; Le Fèvre, R. J. W.; Ras, B. P.; Smith, M. R. *J. Chem. Soc.* **1959**, 1188.
(72) (a) de Melo, C. P.; Silbey, R. *J. Chem. Phys.* **1988**, *88*, 2558. (b) de Melo, C. P.; Silbey, R. *J. Chem. Phys.* **1988**, *88*, 2567.
(73) Nakano, M.; Okumura, M.; Yamaguchi, K.; Fueno, T. *Mol. Cryst. Liq. Cryst.* **1990**, *182A*, 1.
(74) (a) Churchill, J. N.; Holmstrom, F. E. *Am. J. Phys.* **1982**, *50*, 848. (b) Churchill, J. N.; Holmstrom, F. E. *Phys. B* **1983**, *123*, 1.
(75) Callaway, J. In *Energy Band Theory*; Academic Press: New York, 1964; p 277.
(76) (a) Agrawal, G. P.; Flytzanis, C. *Chem. Phys. Lett.* **1976**, *44*, 366. (b) Cojan, C.; Agrawal, G. P.; Flytzanis, C. *Phys. Rev.* **1977**, *B15*, 909. (c) Agrawal, G. P.; Cojan, C.; Flytzanis, C. *Phys. Rev. Lett.* **1977**, *38*, 711. (d) Agrawal, G. P.; Cojan, C.; Flytzanis, C. *Phys. Rev.* **1978**, *B17*, 776.
(77) (a) Barbier, C. *Chem. Phys. Lett.* **1987**, *142*, 53. (b) Barbier, C.; Delhalle, J.; Andrê, J. M. In *Nonlinear Optical Properties of Polymers*; Heeger, A. J., Orenstein, J., Ulrich, D. R., Eds.; Materials Research Society: Pittsburgh, 1988; p 239. (c) Barbier, C.; Delhalle, J.; Andrê, J. M. *J. Mol. Struct. (THEOCHEM)* **1989**, *188*, 299. (d) Champagne, B.; Andrê, J. M. *Int. J. Quantum Chem., Quantum Chem. Symp.* **1990**, *24*, 859. (e) Andrê, J. M.; Champagne, B. In *Organic Molecules for Nonlinear Optics and Photonics*; Messier, J., Kazjar, F., Prasad, P., Eds.; Kluwer Academic Publishers: Dordrecht, 1991; p 1. (f) Champagne, B.; Andrê, J. M. *Int. J. Quantum Chem.* (issue in honour of E. Clementi), accepted.
(78) Genkin, V. M.; Mednis, P. M. *Sov. Phys.-JETP* **1968**, *27*, 609.
(79) (a) Ladik, J. *Acta Phys. Hung.* **1965**, *18*, 173. (b) Ladik, J. *Acta Phys. Hung.* **1965**, *18*, 185. (c) Andrê, J. M.; Gouverneur, L.; Leroy, G. *Int. J. Quantum Chem.* **1967**, *1*, 427. (d) Andrê, J. M.; Gouverneur, L.; Leroy, G. *Int. J. Quantum Chem.* **1967**, *1*, 451. (e) Del Re, G.; Ladik, J.; Biczo, G. *Phys. Rev.* **1967**, *155*, 997. (f) Andrê, J. M. *J. Chem. Phys.* **1969**, *50*, 1536. (g) Andrê, J. M. *Adv. Quantum Chem.* **1980**, *12*, 65.
(80) (a) Ladik, J. *Quantum Theory of Polymers as Solids*; Plenum Press: New York; 1988. (b) Andrê, J. M.; Delhalle, J.; Brêdas, J. L. *Quantum Chemistry Aided Design of Organic Polymers for Molecular Electronics*; World Scientific Publishing Company: Singapore, 1991.

(81) Jones, W.; March, N. H. In *Theoretical Solid State Physics*, J. Wiley & Sons: London, Vol. 2, 1973, p 800.
(82) Ueno, N.; Seki, K.; Fujimoto, H.; Kuramochi, T.; Sigita, K.; Inokuchi, H. *Phys. Rev.* **1990**, *B41*, 1176.
(83) Teramae, H.; Takeda, K. *J. Am. Chem. Soc.* **1989**, *111*, 1281.
(84) Tanaka, K.; Yamashita, S.; Yamabe, T. *Macromol.* **1986**, *19*, 2062.
(85) Risser, S. M.; Ferris, K. F. *Chem. Phys. Lett.* **1990**, *170*, 349.
(86) Tokura, Y.; Koda, T.; Itsubo, A.; Miyabayashi, M.; Okuhara, K.; Ueda, A. *J. Chem. Phys.* **1986**, *85*, 99.